REVIEW

Anticancer drug discovery by targeting cullin neddylation

Qing Yu[a], Yihan Jiang[a], Yi Sun[a,b],*

[a]*Cancer Institute of the 2nd Affiliated Hospital, Institute of Translational Medicine, Zhejiang University School of Medicine, Hangzhou 310029, China*
[b]*Division of Radiation and Cancer Biology, Department of Radiation Oncology, University of Michigan, Ann Arbor, MI 48109, USA*

Abstract Protein neddylation is a post-translational modification which transfers the ubiquitin-like protein NEDD8 to a lysine residue of the target substrate through a three-step enzymatic cascade. The best-known substrates of neddylation are cullin family proteins, which are the core component of Cullin −RING E3 ubiquitin ligases (CRLs). Given that cullin neddylation is required for CRL activity, and CRLs control the turn-over of a variety of key signal proteins and are often abnormally activated in cancers, targeting neddylation becomes a promising approach for discovery of novel anti-cancer therapeutics. In the past decade, we have witnessed significant progress in the field of protein neddylation from pre-clinical target validation, to drug screening, then to the clinical trials of neddylation inhibitors. In this review, we first briefly introduced the nature of protein neddylation and the regulation of neddylation cascade, followed by a summary of all reported chemical inhibitors of neddylation enzymes. We then discussed the structure-based targeting of protein−protein interaction in neddylation cascade, and finally the available approaches for the discovery of new neddylation inhibitors. This review will provide a focused, up-to-date and yet comprehensive overview on the discovery effort of neddylation inhibitors.

1. Introduction

Ubiquitin−proteasome system (UPS) plays a vital role in the maintenance of cellular homeostasis[1]. Ubiquitylation is catalyzed by a cascade of three enzymes: E1 activating enzymes, E2 conjugating enzymes, and E3 ligases to sequentially transfer ubiquitin to the substrate proteins[2−6]. The consequence of a protein conjugated with a single ubiquitin or polyubiquitin chains can be manifold, involving a panel of biological activities, including but not limited to proteasomal degradation, and regulation of DNA replication and repair, cell signaling, endocytosis, or immune response, among the others[7−10]. Therefore, the dysfunction of UPS can lead to a variety of diseases, including metabolic syndromes, neurodegeneration and cancer[11].

It has been over two decades since the discovery that proteasome inhibitors could induce apoptosis in human cancer cells[12,13]. Many follow-up studies further validated that the UPS is a promising anticancer target, eventually leading to U.S. Food and Drug Administration (FDA) approval of a landmark proteasome inhibitor, bortezomib (velcade), for the treatment of multiple myeloma and relapsed mantle cell lymphoma[14,15]. Due to high cytotoxicity of general inhibitor of the UPS, the subsequent efforts have been extended to target the upstream ubiquitin enzymes with more selectivity for cancer cells and less toxicity against normal cells.

Protein neddylation, like ubiquitylation, is also catalyzed by three-enzyme cascade, leading to attachment of ubiquitin-like NEDD8 (neural precursor cell-expressed developmentally down-regulated 8) to a substrate protein on a lysine residue[16]. These enzymes are the E1 NEDD8-activating enzyme (NAE), E2 NEDD8-conjugating enzyme and E3 NEDD8 ligase[16]. The best-characterized substrates of neddylation are the cullin family members, the scaffold components of cullin−RING E3 ubiquitin-ligases (CRLs), which mediate the final step of ubiquitin transfer to a substrate, thus determining the efficiency and substrate selectivity of the ubiquitylation cascade[17]. Neddylation activates CRLs to promote the ubiquitylation and degradation of their substrates, of which many are tumor suppressive proteins[18−21]. Thus, targeting neddylation in cancer cells would inactivate CRLs to cause accumulation of tumor suppressor substrates, thus becoming a sound strategy for anticancer therapy[22−27]. Note that in this review, "neddylation" refers to "cullin neddylation", unless otherwise specified.

In 2009, the discovery and subsequent clinical trials of an NAE inhibitor MLN4924 (pevonedistat)[26] set a milestone that validated neddylation pathway as an effective anticancer target. The continuous effort has been made thereafter to seek for more drug-like neddylation inhibitors. Now a decade later, high-throughput screening, virtual screening, as well as structural-based design have yielded a diverse collection of small-molecule inhibitors of neddylation, and some showed promising anticancer activities. In this review, we will briefly introduce the recent progress in the regulation of neddylation cascade, followed by a summary of all reported chemical neddylation inhibitors. We will then discuss potential opportunity in targeting the protein−protein interaction in neddylation cascade, and finally the available approaches for discovery of new drug candidates in targeting neddylation.

2. The enzymatic cascade of neddylation and its regulation

Neddylation in many ways resembles ubiquitylation. Among the 16 reported human ubiquitin-like proteins (UBLs)[28], NEDD8 has the highest structural similarity with ubiquitin (59% identical)[29].

Similar to ubiquitin, mature NEDD8 has a Gly−Gly sequence at the end of its carboxy-terminal tail which is covalently attached to a lysine residue in the target protein[30]. Despite the similarities, NEDD8 and ubiquitin have some small differences in the less conserved regions including the intervening polar and charged surfaces, which may be the key factors to affect their own functions[16]. While ubiquitin is conjugated to substrates mainly through specific-lysine-linked poly-ubiquitin chains (e.g., poly-ubiquitin chains via K11, K48 or K63-linkage), NEDD8 is mostly found conjugated to a single Lys residue on a substrate with mono-NEDD8[31]. Functionally, substrates conjugated with the canonical K48-linked poly-ubiquitin chains are doomed for degradation, whereas NEDD8-conjugate substrates undergo the conformational changes, leading to altered functions (discussed below). Just like ubiquitylation, neddylation is catalyzed by a stepwise enzymatic cascade with its own E1, E2s and E3s (Fig. 1). First, NAE, a heterodimer that consists of amyloid-β precursor protein binding protein 1 (APPBP1) and ubiquitin-activating enzyme 3 (UBA3), activates NEDD8 in an ATP-dependent manner[32]. NEDD8 first binds to the adenylation site of UBA3 with MgATP[32] and yields NEDD8−AMP[33]. The C-terminus of NEDD8 then reacts with the catalytic cysteine of NAE to form an NAE−NEDD8 thioester and to release AMP[34]. A second NEDD8 then binds at the adenylation site and yields a second NEDD8−AMP, forming a ternary complex that contains two NEDD8 molecules bound to NAE[34]. Subsequently, one of the two NEDD8 E2 conjugating enzymes, UBE2M (also known as UBC12)[35], or UBE2F[36] binds to the NAE−NEDD8 complex and catalyzes a trans-thiolation reaction to transfer thioester bound NEDD8 to the active site cysteine of the E2 enzyme. In the final step, NEDD8 E3 ligases catalyzes the transfer of NEDD8 from E2 to the target protein[37]. Most reported NEDD8 E3 ligases contain RING domain[5], among which the best-studied are the RING domain subunits RING-box protein 1 (RBX1) (also known as regulators of cullins 1, ROC1) and its homologue RBX2 (also known as ROC2 or sensitive to apoptosis gene SAG)[5]. RBX1 preferentially interacts with UBE2M to neddylate several members of cullin family, including cullin-1, -2, -3, -4A and -4B, while RBX2 couples with UBE2F to specifically neddylate cullin 5[36,38,39].

Several proteins have been described to regulate neddylation by distinctive mechanism. In yeast, DCN1 (defective in cullin neddylation 1 protein) is the best-studied regulator of cullin-neddylation[40]. DCN1 binds both cullins and the acetylated N-terminus of the UBE2M and functions as a scaffold-like co-E3-ligase to direct NEDD8 towards the right lysine residue on cullins and thus promotes neddylation[41−44]. A recent study demonstrated that glycyl-tRNA synthetase (GlyRS), an essential enzyme in protein synthesis, interacts with NEDD8, NEDD8 E1 and UBE2M E2 to critically enhance the neddylation[45]. Specifically, GlyRS binds to APPBP1 subunit of NEDD8 E1 through its ABD domain, and captures and specifically binds UBE2M, but not UBE2F, before the E2 reaches a downstream E3 ligase. Tfb3 is another regulator found in yeast controlling the conjugation step of cullin neddylation[46]. Tfb3 also has a RING domain, physically interacts with Ube2M and the Hrt1/Rtt101 E3 complex (note that Hrt1 is yeast RBX1, Rtt101 is a yeast version of cullin-4), and critically promotes Rtt101 neddylation. In addition, Tfb3 regulates the neddylation and activity of cullin-3, but not the culllin-1 ortholog Cdc53[46]. Most recently, we found an interesting cross-talk between two neddylation E2s. Specifically, UBE2M, upon induced by stresses, such as hypoxia or tumor promoter TPA (12-O-tetradecanoylphorbol-13-acetate), acts as dual E2 for cullin-3
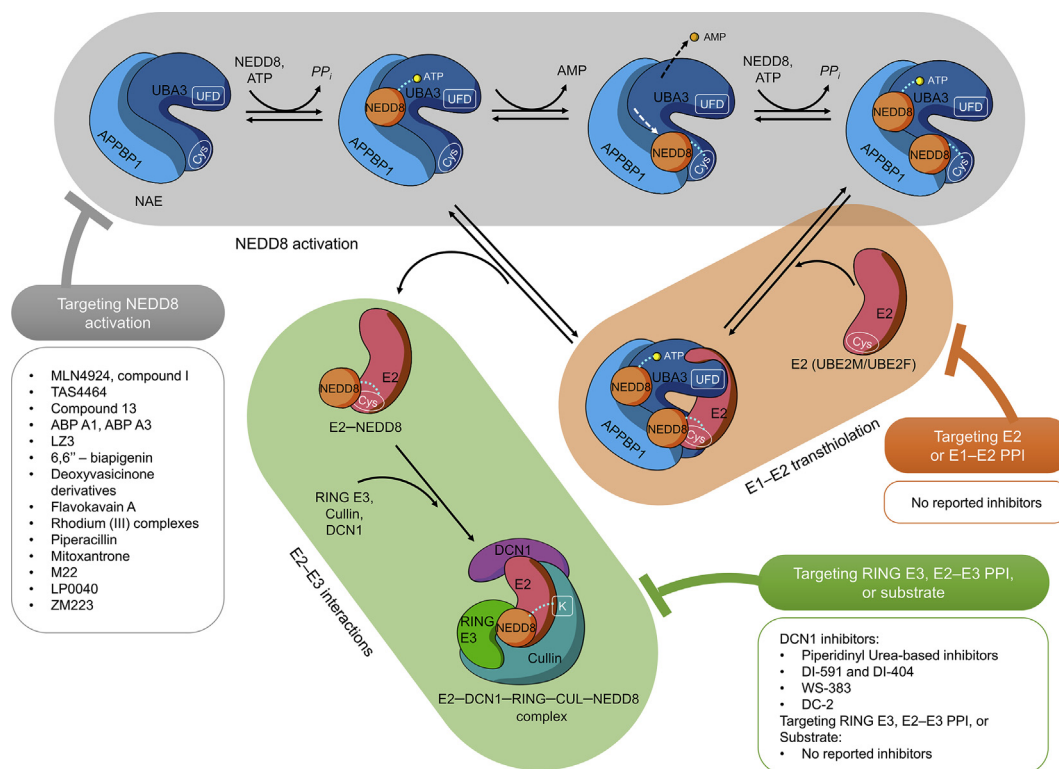
Figure 1 The neddylation cascade and inhibiting strategies. Neddylation is a stepwise enzymatic cascade. NEDD8 first binds to the adenylation site of UBA3 with MgATP. The C-terminus of NEDD8 then reacts with the catalytic cysteine of UBA3 to form an NAE−NEDD8 thioester and release AMP. A second NEDD8 then binds at the adenylation site and forms a ternary complex that contains two NEDD8 molecules bound to NAE. Subsequently, a NEDD8 E2 binds to the NAE−NEDD8 complex and catalyzes a transthiolation reaction to transfer thioester-bound NEDD8 to the active site cysteine of the E2 enzyme. Finally, a NEDD8 E3 ligases catalyzes the transfer of NEDD8 from E2 to a specific lysine residue of target protein. Targeting each step in neddylation cascade is shown with available compounds listed. Note that the illustration was created based on following crystal structures: 2NVU, 1YOV, 1Y8X and 4P5O.

neddylation and Parkin E3 ligase to promote ubiquitylation and degradation of UBE2F[47].

3. Inhibitors of neddylation enzymes

Since the best characterized function of neddylation modification is to activate CRLs, which then ubiquitylate a variety of tumor suppressor substrates for proteasomal degradation in human cancer cells, neddylation process has been validated as an attractive cancer target[24]. Indeed, the process of neddylation is abnormally activated due to overexpression of NEDD8, and several neddylation enzymes, including APPBP1/UBA3, UBE2M, UBE2F, DCN1, RBX1, and SAG in multiple types of human cancers, such as carcinomas in the lung, liver, and colon, glioblastoma, and esophageal squamous cell carcinoma[48−56]. Moreover, the elevated status of these neddylation enzymes is related to poor patient prognosis[49,51,53,55,56]. Taken together, these studies provide strong evidence that neddylation modification is a promising anticancer target. In this section, we will review the currently reported inhibitors of neddylation enzymes for anticancer application.

3.1. NAE inhibitors

NAE initiates the neddylation cascades in an ATP-dependent manner. There are three important domains in NAE, an active adenylation domain in UBA3 for acyladenylate formation, a

catalytic cysteine transthiolation domain to form E1−NEDD8 thioesters, and a C-terminal ubiquitin fold domain (UFD) for E2 interaction[34,57−59]. The structure-based studies of neddylation E1, E2 and their interactions[47] revealed multiple approaches, at least in theory, to discover the inhibitors of the NEDD8 activating step: 1) to prevent ATP from binding to the active adenylation site in NAE with ATP-competitive inhibitors, which is a strategy widely used to inhibit kinases[60]; 2) to mimic the NEDD8−AMP intermediate by the formation of a NEDD8−compound adduct, resembling NEDD8 adenylate, but to block subsequent intra-enzyme reactions[61] (e.g., MLN4924, see below). Similar strategy has been applied for few other adenylate-forming enzymes[62]; or 3) to block the formation of E1−NEDD8 thioesters by targeting the active-site cysteine in E1 (e.g., the UAE inhibitor PYR-41)[63]; and 4) to block the transfer of NEDD8 to an E2 by interrupting E1−E2 interaction. Most of the current NAE inhibitors are reported to exert their inhibitory effect through the first two modes, as discussed below (Table 1).

3.1.1. MLN4924
MLN4924 (Fig. 2A, #1), the first-in-class inhibitor that specifically targets NAE, was identified through a high-throughput screening (HTS), followed by iterative medicinal chemical improvement in 2009[26]. MLN4924 showed potent and highly selective inhibitory effect against NAE by blocking the formation of E2−NEDD8 thioesters in purified enzyme assays with an IC$_{50}$

Table 1 Reported inhibitors of NAE.[a]

ID	Name	Target	Enzyme assay, IC_{50}[b]	Cellular neddylation, IC_{50}	Cell growth, EC_{50}	Cell line[c]	Accumulated CRL substrate	Clinical trial	Year	Ref.
Covalent inhibitor										
#1	MLN4924 (pevonedistat)	NAE	4 nmol/L	<10 nmol/L[e]	0.1 ± 0.02 μmol/L	HCT-116 (colorectal)	CDT1, P27, NRF2, c-Jun, HIF1α, et al.	Phase I/II	2009	26
#2	Compound I	Pan-E1	2.8 ± 0.2 μmol/L	NA	NA	HCT-116 (colorectal)	NA	NA	2011	73
#3	TAS4464	NAE	0.995 nmol/L	<1 nmol/L[e]	<10 nmol/L[e]	CCRF-CEM (ALL)	CDT1, P27, p-IκBα, NRF2	Phase I	2019	77
#4	Compound 13	NAE	<10 nmol/L	<50 nmol/L[e]	160 ± 88 nmol/L	K562 (leukemia)	N/A	NA	2011	74
#5	ABP1	Pan-E1	<10 μmol/L[e]	NA	NA	NA	NA	NA	2013	82
#6	ABP A3	NAE, UAE	<0.1 μmol/L[e]	<12.5 μmol/L[e]	2.5 μmol/L	A549	P53, P27	NA	2015	83
#7	LZ3	NAE[d]	1.06 ± 0.18 μmol/L	<1.88 μmol/L[e]	12.3−29.5 μmol/L	Caco-2, MCF-7, Bcl-7402	NA	NA	2014	84
Non-covalent inhibitor										
#8	6,6″-Biapigenin	NAE[d]	20 μmol/L	5 μmol/L	NA	Caco-2	NA	NA	2011	85
#9	Deoxyvasicinone derivative	NAE	0.8 μmol/L	6 μmol/L	10 μmol/L	Caco-2	P27[kip1]	NA	2012	86
#10, 11	Deoxyvasicinone derivatives	NAE	<1.25 μmol/L[e]	0.27−0.39 μmol/L	NA	Caco-2	P27, CDT1	NA	2015	87
#12	Flavokawain A	NAE[d]	5 μmol/L	<40 μmol/L[e]	NA	PC3	NA	NA	2015	88
#13	[Rh(ppy)$_2$(dppz)]$^+$	NAE	1.5 μmol/L	<1.56 μmol/L[e]	0.3 μmol/L	Caco-2	IκBa, P27	NA	2012	89
#14	[Rh(phq)$_2$(MOPIP)]$^+$	NAE	0.1 μmol/L	NA	4.3 μmol/L	Caco-2	β-Catenin, IκBα, c-Myc, NRF2, CDT1	NA	2017	90
#15	Piperacillin	NAE	1 μmol/L	<13.5 μmol/L[e]	NA	Caco-2	P27[kip1]	NA	2014	91
#16	Mitoxantrone	NAE	NA	1.3 μmol/L	1.4 μmol/L	Caco-2	P53, P27	NA	2018	92
#17	M22	NAE	<10 μmol/L[e]	<10 μmol/L[e]	5.5 μmol/L	A549	CDT1, P27, P53	NA	2016	93
#18	LP0040	NAE, UAE	<3.33 μmol/L[e]	<6 μmol/L[e]	0.76 ± 1.26 μmol/L	AGS	P27, CDT1, NRF2	NA	2018	94
#19	ZM223	NAE[d]	NA	NA	0.1−1.22 μmol/L	HCT-116, U-2OS	NA	NA	2017	95

NA: not available.

[a]Data was collected only from cited references.

[b]There are variations in the methods of enzyme assays across the publications.

[c]The cell lines used to generate the IC_{50} and EC_{50} in the left two columns.

[d]No evidence for selectivity over the other E1s was shown in cited references.

[e]Data was roughly estimated by visual inspection of the gels presented in cited references.
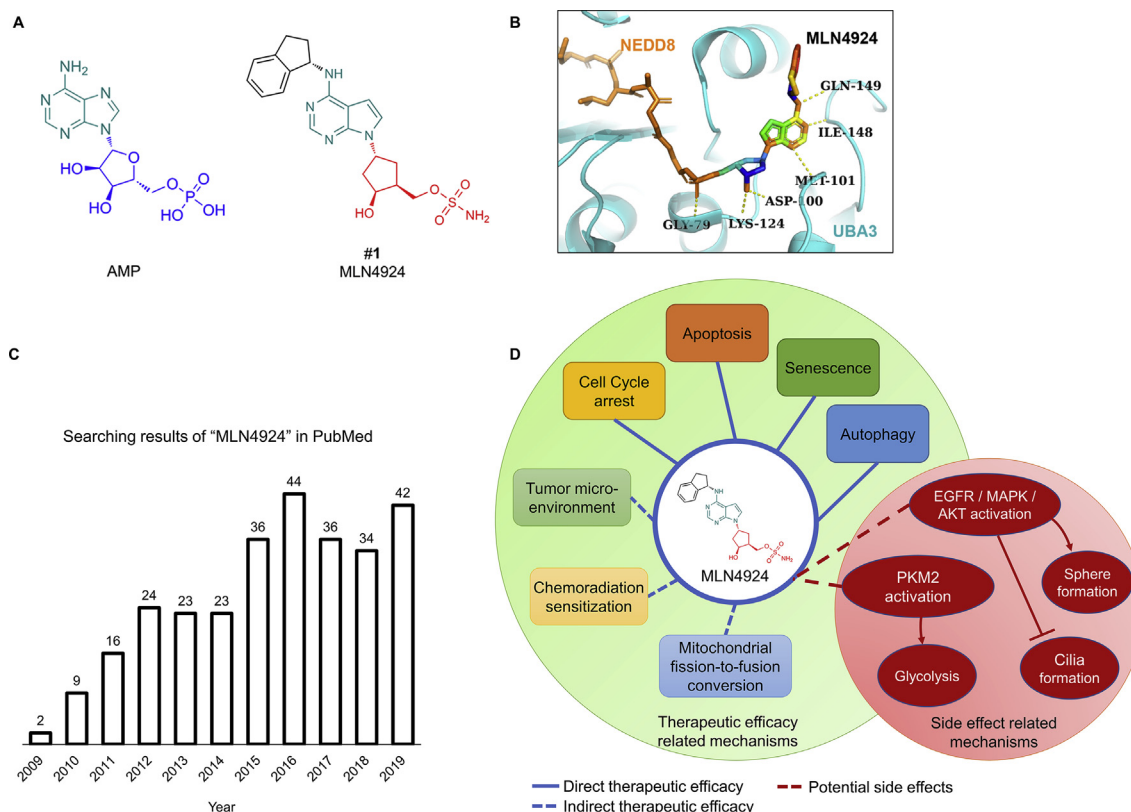
Figure 2 The first-in-class NAE inhibitor, MLN4924. (A) Chemical structure of adenosine 5′-monophosphate (AMP) and MLN4924; (B) co-crystal structure of MNL4924 and NAE (PDB: 3GZN); (C) the number of MLN4924 publications each year for the past decade, data was last updated on 16 August, 2019; (D) a scheme of the mechanisms of MLN4924 regarding to its therapeutic efficacy and side effect.

of 4 nmol/L[26]. In a wide varieties of cancer cell lines, MLN4924 completely inhibited the neddylation of all cullins at nanomolar to low micromolar range and causes accumulation of many tumor suppressor substrates, leading to remarkable suppression of growth and survival, and sensitization of chemo-radiation by inducing growth arrest, apoptosis, senescence and autophagy[24,26]. In many *in vivo* xenograft tumor models, MLN4924 effectively suppressed tumor growth and metastasis with well-tolerated toxicity[26]. These promising preclinical findings advanced MLN4924 into a series of Phase I and II clinical trials in patients with melanoma, lymphoma, AML, MDS, and multiple solid tumors, alone or in combination with conventional chemotherapies[64−68].

The crystal structure of NAE−NEDD8−MLN4924 complex (PDB: 3GZN) was published in 2011[61], which showed the mechanism of MLN4924 action against NAE. Specifically, MLN4924 with structure similarity to adenosine 5′-monophosphate (AMP) forms a very stable adduct with NEDD8 in an NAE-MgATP dependent manner. The NEDD8−MLN4924 adduct within the NAE active site prevents the transfer of NEDD8 to E2, and therefore potently inhibits neddylation cascade[61]. Crystal structure showed that the binding of MLN4924 to NEDD8 and NAE did not affect the orientations of the catalytic cysteine domain or the UFD domain[61]. In fact, the conformation of NAE bound with NEDD8 and MLN4924 closely resembles those with NEDD8 and ATP. Comparison of the NAE−NEDD8−MgATP structure in the absence or presence of MLN4924 revealed several important NAE−ATP interaction sites located in the adenylation domain of NAE, including the side chains of Asp100 and Lys124,

the backbone amide NH of Ile 148 and the side chain of Gln149[61] (Fig. 2B).

Although AMP-mimetics can potently inhibit ATP-related enzymes was nothing new[69], and an adenylate analog was previously reported as a specific inhibitor of UAE[70], the discovery of MLN4924, a highly selective inhibitor of neddylation E1, has far more impacts than a simple adenosine sulfamate-like compound, as clearly evidenced by a PubMed search under the keyword "MLN4924", which yielded 289 publications (as of 16 August, 2019) since its first publication 10 years ago (Fig. 2C).

Biologically, as a mechanism-based small-molecule inhibitor specifically targeting neddylation, MLN4924 has become a useful tool in studying the role of neddylation in a variety of biological processes, particularly as a novel class of anti-cancer agent (Fig. 2D). MLN4924 inhibits the growth of various cancer cell lines by triggering cell cycle arrest, apoptosis, senescence, and autophagy in a context dependent manner, and sensitizes cancer cells to chemoradiation as well as alters the tumor microenvironment (for recent reviews, see Refs. 24 and 71). MLN4924 studies have also led to some unexpected connection between neddylation and other important cellular processes. For example, we recently unexpectedly found that MLN4924 could induce mitochondrial fission-to-fusion conversion and alter mitochondrial functions in breast cancer cells, linking neddylation to energy metabolism[72].

Biochemically, high selectivity of MLN4924 towards NAE over the other E1s (for ubiquitylation or sumoylation) is a remarkable finding, given the fact that most E1s share highly conserved structures and very similar mechanism for the

activation of UBLs. An analog of MLN4924, designated as compound I (Fig. 3B, #2), was also an adenosine sulfamate. Like MLN4924, compound I inhibited E1-dependent ATP-PPi exchange activity through covalent adduct formation (Fig. 3A), but had non-selective inhibitory activity against neddylation E1, as compared to all other E1s[73]. By comparing the inhibitory efficiency of the compound and the purified compound-UBL adduct, it appears that the adduct formation rate and the adduct-E1 binding affinity are the two key factors contributing to the potency. One follow-up study further suggested that the purine C6 position on compound I maybe a determinant for selectivity[74]. Further investigations on the non-conserved region in the nucleotide binding domain of different E1s and related modification on the adenosine sulfamate scaffold may eventually elucidate the true determinants of selectivity, which will lay the ground work for future discovery of small molecules selectively targeting each E1.

Structure-wisely, the mode of MLN4924 action against NAE has triggered extensive searches for additional small-molecules or probes targeting NAE (discussed below). Most of these studies used one of the following strategies: 1) structure-based design with reference to the structure of MLN4924 or compound I, or **2**) virtual screening based on the crystal structure of NAE−NEDD8−MLN4924 (PDB: 3GZN). However, none of the modified compounds shows any significantly improvement over

MLN4924 in biochemical or biological assays, and MLN4924 remains the only and best NAE inhibitor currently in several clinical trials.

Despite these positive impacts, MLN4924 has also shown some expected or unexpected downsides. First, it inhibits neddylation E1 to block the entire neddylation modification in cells, thus having inherited and unavoidable cytotoxicity. This feature, however, inspired drug discovery efforts to target downstream E2s or E3s for enhanced specificity and reduced toxicity. Second, general inhibition of neddylation of all cullin family members likely neutralizes some anti-cancer effects by causing accumulation of both suppressive and oncogenic substrates in cell context dependent manner. Third, our recent studies have shown some potential "off-target" effects of MLN4924. We found that MLN4924 at nanomolar concentration triggered EGFR dimerization, leading to activation of MAPK and PI3K/AKT signals to significantly stimulate stem cell proliferation, self-renewal and differentiation in both tumor and normal stem cell models[75]. MLN4924 also promoted *in vivo* tumorigenesis, if mixed with tumor cells at time of inoculation in a xenograft tumor model, and enhanced EGF-mediated wound healing in mouse skin[75]. Furthermore, MLN4924-induced AKT1 activation was causally related to the blockage of ciliogenesis and promotion of cilia disassembly[76]. On the other hand, MLN4924 triggered the
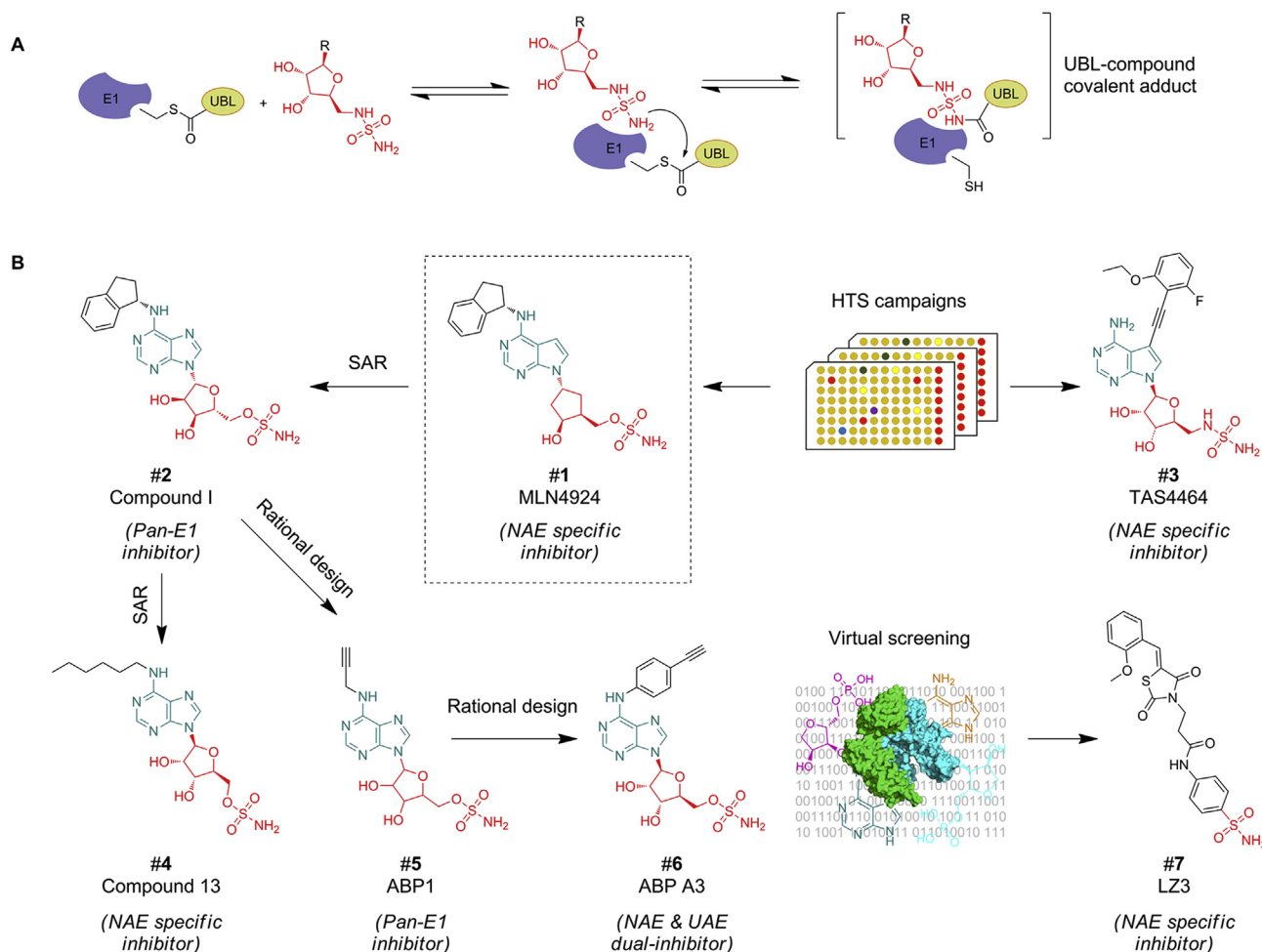

Figure 3 Chemical structures and the mode of action of reported covalent inhibitors targeting NAE. (A) The mode of action of covalent NAE inhibitors; (B) the chemical structures and the developing process of reported covalent inhibitors targeting NAE.

tetramerization of PKM2 to activate glycogenesis and promote mitochondrial oxidative phosphorylation (OXPHOS)[72]. Treatment of MLN4924 in combination with metformin (as an OXPHOS inhibitor) or shikonin (as a glycolysis inhibitor) could synergistically inhibit the growth of breast cancer cells *in vitro* and *in vivo*[72]. These findings provide sound rationale for effective combinational therapy to enhance the efficacy of MLN4924. Finally, poor efficacy of MLN494 in some patients when applied as a single agent has been observed[64,65,67], which could be due to lack of neddylation activation in the tumor tissues of these patients or the "side-effects" described above. Nevertheless, neddylation biomarkers (*e.g.*, increased E1 levels) should be developed and used as an important screening approach in the stage of patient recruitment to ensure therapeutic efficacy of neddylation inhibitors.

3.1.2.   Other covalent NAE inhibitors

Several small-molecule inhibitors targeting NAE through covalent binding have been reported. Structurally, all these compounds comprised the sulfamate group similar to MLN4924, with expectation to form a covalent adduct with the carboxyl terminus of NEDD8. Most of the compounds also retained the adenosine group to mimic ATP (Fig. 3). Accordingly, all these molecules were expected to exhibit a similar mode of action assembling MLN4924. Below we discuss the highlighted properties of each inhibitor with more information listed in Table 1.

3.1.2.1.   Adenosine sulfamate analogs.
TAS4464 (Fig. 3B, **#3**), a small molecule developed by Taiho Pharmaceuticals *via* HTS and structure-based design, was recently published with claimed inhibitory effects greater than MLN4924 in certain cell lines[77]. In an *in vitro* parallel UBE2M−NEDD8 thioester forming assay, TAS4464 selectively inhibited NAE with an IC_{50} of 0.995 nmol/L, ten times better than MLN4924 (10.5 nmol/L). At the cellular level, TAS4464 inhibited neddylation and accumulated CRL substrates CDT1, NRF2, p-IκBα, and P27 with lower effective concentration than that of MLN4924[78−81]. In terms of cytotoxicity against cancer cells, TAS4464 showed 3−64−folds higher potency than MLN4924 in multiple cell lines tested. In the *in vivo* assay, TAS4464 showed a wide therapeutic window in multiple xenograft mouse models, including CCRF-CEM (human acute lymphoblastic leukemia), GRANTA-519 (mantle cell lymphoma), SU-CCS-1 (human clear cell sarcoma) and LU5266 (small cell lung cancer). A spotlighted feature of TAS4464 was that it showed lower risk of electrolyte abnormalities caused by Carbonic anhydrase II (CA2) in red blood cells, which was observed with MLN4924[64], suggesting potentially less side effect for TAS4464 treatment. A search in ClinicalTrials.gov revealed that TAS4464 entered a Phase I clinical trial for patients with multiple myeloma or lymphoma in 2016 (NCT02978235). The trial was, however, terminated surprisingly due to "business decision" in 2018 without any clinical data disclosed.

In 2011, Julie et al.[73] pursued the structural determinants of NAE selectivity based on the structure of compound I. Through the virtual docking of compound I within the ATP pocket of NAE (PDB: 3GZN), the authors found a "gate-keeper" region above the ATP pocket which could be well occupied by the 2,3-dihydroindene moiety present in both compound I and MLN4924[74]. Taken this region as the "hotspot", the authors designed and synthesized a series of analogs of compound I with *N*-alkyl groups at purine C6. This structure−activity relationship

(SAR) study identified a set of inhibitors with sub-10 nmol/L NAE-specific inhibitory effect. Among them, compound **13** (Fig. 3B, **#4**) showed a comparable potency as MLN4924 in K562 leukemia cells[74].

In 2013, based on the structure of compound I, An et al.[82] designed ABP1 (Fig. 3B, **#5**), an analog of compound I with the indane moiety substituted by a propargyl group. ABP1 could form a covalent adduct with UBL in the same way as compound I or MLN4924. The innovation point is that the UBL ABP1 adduct could be readily conjugated to a fluorescent tag or a biotin tag by click chemistry. ABP1 could, thus, serve as an activity-based probe to detect or monitor E1 activity *in vitro* and inside intact cells[82]. On the base of ABP1, the group further designed ABP A3 (Fig. 3B, **#6**), as a dual inhibitor of both Ub E1 and NEDD8 E1[83]. ABP A3 selectively decreased ubiquitin and NEDD8 conjugates, but not SUMO1−3, Ufm1, ISG15 or LC3 conjugates in A549 cells.

3.1.2.2.   Sulfamate-containing, non-adenosine like inhibitor.
In 2014, Zhang et al.[84] used a novel strategy by combining covalent docking and virtual screening which incorporated both ligand-based and structure-based pharmacophore modeling. Three covalent inhibitors of NAE were identified, among which LZ3 showed most potent inhibitory activity in *in vitro* assays (Fig. 3B, **#7**). LZ3 was designed to retain the sulfamoyl group which was required for covalent binding with the Gly76 of NEDD8. A cell-based washout experiment supported the covalent binding mechanism for LZ3[84]. Covalent docking model predicted that LZ3 bond to NAE with a similar pattern as MLN4924, and SAR study indicated that its phenylamino group, which was predicted to interact with the Asp100 in the adenylation site, was crucial for maintaining the binding affinity.

3.1.3.   Non-covalent ATP-competitive inhibitors

A variety of reversible NAE inhibitors was also reported by different groups through virtual screening or structure-based design (Fig. 4). The *in vitro* enzyme assays showed that these compounds had moderate to potent activity for NAE inhibition, and all but one showed selectivity towards NAE over other E1s. While these non-sulfamide molecules showed no evidence of covalent binding to NAE or NEDD8, molecular docking models predicted that they might competitively interrupt E1−NEDD8−ATP interaction by forming hydrogen bonds (H-bonds) within the ATP binding site, though the binding poses varied through different compounds. Most of the compounds were tested in select cancer cell lines and some showed potent cytotoxic effect at micromolar range with consistent inhibitory effect against cullin neddylation. Below we discuss the highlighted properties of each inhibitor with additional information listed in Table 1.

3.1.3.1.   Natural products.
In 2011, Leung et al.[85] identified 6,6″-biapigenin (Fig. 4, **#8**) as the first natural-product like NAE inhibitor through virtual screening. Molecular modeling analysis suggested that 6,6″-biapigenin and MLN4924 had a different binding pose in the NAE−NEDD8 complex. Specifically, 6,6″-biapigenin might situated closer to the APPBP1 subunit and interacts with NEDD8, forming multiple H-bonding interactions with UBA3, APPBP1 and NEDD8.

A dipeptide-conjugated deoxyvasicinone derivative (Fig. 4, **#9**) was also identified by the virtual screening with potent inhibitory
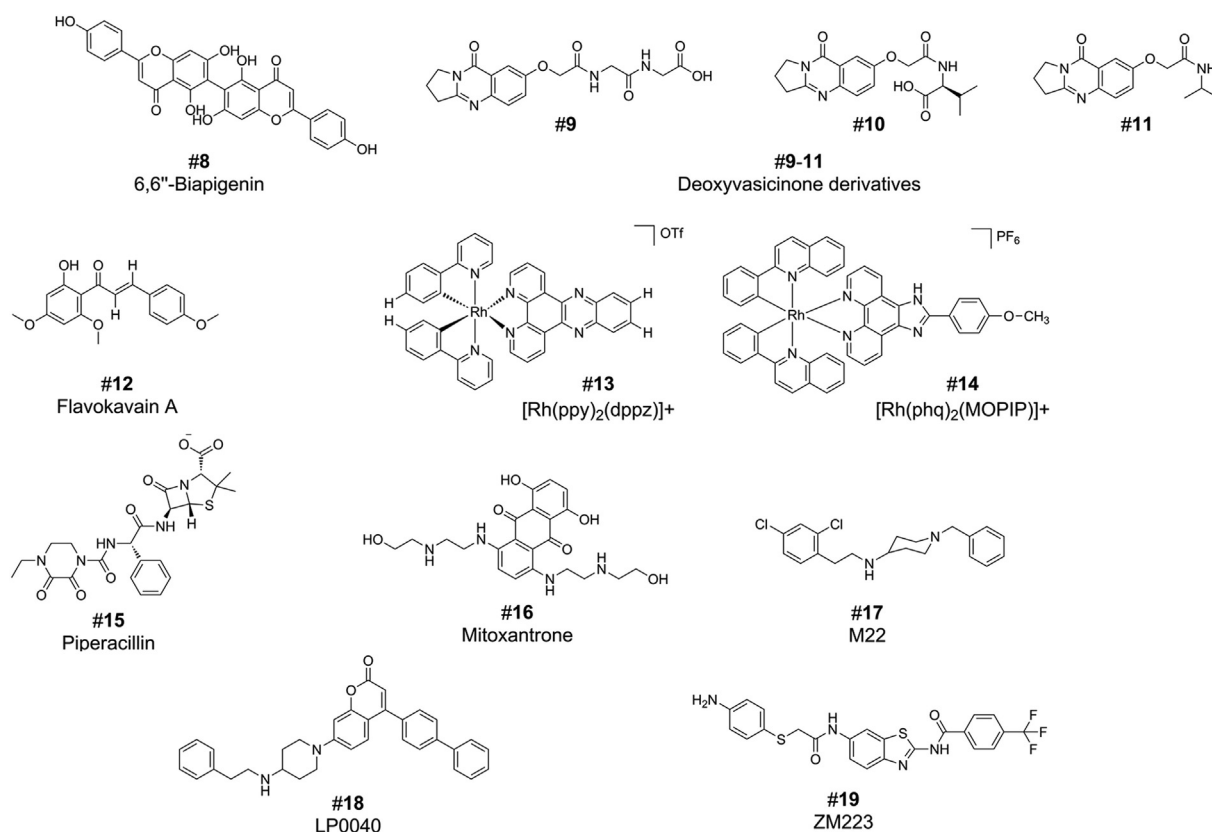
Figure 4   Chemical structures of reported non-covalent inhibitors targeting NAE.

against NAE activity in enzyme assays (IC$_{50}$ = 0.8 μmol/L)[86]. A follow-up pharmacophore screening yielded another two deoxyvasicinone derivatives (Fig. 4, **#10** and **11**) with comparable potency in enzyme assays and stronger cytotoxicity in human epithelial colorectal adenocarcinoma cell line Caco-2 with IC$_{50}$ around 0.27−0.39 μmol/L[87].

Flavokawain A (FKA), a chalcone from the kava plant, was initially found as a potent apoptosis inducer for bladder and prostate cancer cells (Fig. 4, **#12**)[88]. Further studies revealed that FKA actually also inhibited conjugation of NEDD8 to UBE2M and cullin-1 in cells and induced ubiquitination-mediated degradation of S phase kinase-associated protein 2 (SKP2). Docking study indicated that FKA interrupted the ATP binding pocket in NAE. The *in vitro* enzyme assay validated that FKA inhibited the forming of UBE2M−NEDD8 thioester.

3.1.3.2.   Metal complexes.   Two rhodium (III) complexes were identified by structure-based design as metal coordination-complexes that inhibit NAE activity. [Rh(ppy)$_2$(dppz)]$^+$ (Fig. 4, **#13**) had an IC$_{50}$ of 1.5 μmol/L in *in vitro* enzyme assays, and inhibited Caco-2 growth with an IC$_{50}$ of 0.3 μmol/L[89]. [Rh(ppy)$_2$(dppz)]$^+$ exhibited dose-dependent inhibition of UBE2M−NEDD8 thioester levels in Caco-2 cells and caused accumulation of CRL substrates P27^{kip1}. [Rh(phq)$_2$(MOPIP)]$^+$ (Fig. 4, **#14**) showed a much lower IC$_{50}$ in enzyme assays (IC$_{50}$ = 0.1 μmol/L), and exhibited anti-inflammatory activity *in vivo*[90].

3.1.3.3.   FDA-proved drugs.   A virtual screening in a select library containing over 3000 FDA-proved drugs yielded two distinct compounds. Piperacillin (Fig. 4, **#15**) was a semi-synthetic beta-

lactam antibiotic[91], while mitoxantrone (Fig. 4, **#16**) was used as an anthracenedione drug for treating multiple cancers[92]. Both drugs showed *in vitro* inhibitory effect against NAE activity and caused selective accumulation of P27.

3.1.3.4.   Others.   In 2016, Lu et al.[93] identified a 1-benzyl-*N*-(2,4-dichlorophenethyl) piperidin- 4-amine, designated as M22 (Fig. 4, **#17**) with a piperdin-4-amine scaffold, as a reversible NAE inhibitor. M22 inhibited tumor growth in nude mice xenograft model and showed low acute toxicity in zebrafish model. The same group then rationally designed LP0040 (Fig. 4, **#18**), a Ub E1/NEDD8 E1 dual inhibitor[94]. LP0040 showed synergistic effect when combined with bortezomib to inhibit the growth of gastric cell line AGS.

In 2017, Ma et al.[95] conducted a target-based virtual screening, followed by SAR and identified three benzothiazole derivatives as non-covalent non-sulfamide NAE inhibitors, with ZM223 (Fig. 4, **#19**) showing the most potent activity.

3.1.4.   Perspective for further discovery on NAE inhibitors
Even with all these efforts, none of the above reported compounds showed better properties than MLN4924. Indeed, besides MLN4924 and TAS4464, all other reported NAE inhibitors are at the very early stage of development and lack of sufficient data at the cellular or animal levels, not to mention about the clinical trials. Indeed, the sulfonyl-adenosines are truly potent NAE inhibitors, but the room for improvement is limited. It is worth noting that in a patent filed by Millennium Pharmaceuticals. Inc. in 2006, 152 sulfonyl-adenosine-based structures were claimed and among which 112 were claimed to exhibit IC$_{50}$ values less

than or equal to 100 nmol/L in the NAE enzyme Assay[96]. It is conceivable that MLN4924 is the best among these analogs. Thus, it is difficult, if not completely impossible, to identify another sulfonyl-adenosine-based compound that has overwhelmingly advantages over MLN4924 in terms of both potency and selectivity.

In addition, while the non-sulfonyl-adenosine ATP-competitive inhibitors are promising, the current reported inhibitors lack the convincing data on potency or selectivity. Furthermore, most of these compounds were identified through virtual screening or structure-based design. The compound−NAE binding was predicted via computer-aided docking method without confirmation by various binding assays (e.g., isothermal titration calorimetry, biolayer interferometry, or cellular thermal shift assays). Some of the compounds lacked evidence showing selectivity over NAE. On cellular level, most of these compounds were tested in only one cell line. And some of these studies did not provide orthogonal experimental data to demonstrate a true on-target modulation. All these factors restrict the further development of these compounds as the leads.

Taken together, it appears that targeting NAE E1 has its limitation, and future efforts should be more directed to identify inhibitors against neddylation E2s or E3s for better selectivity with anticipated lower toxicity.

3.2.   Inhibitors targeting UBE2M−DCN1 interaction

Mammalian cells express 5 family members of DCN1-like proteins (defective in cullin neddylation protein 1-like proteins, DCNLs), DCNL1−5 (also known as defective in cullin neddylation 1 domain-containing protein 1−5, DCUN1D 1−5)[54,97−100]. The DCNL proteins have distinct amino-terminal domains, but share a conserved C-terminal potentiating neddylation (PONY) domain for direct binding to cullins[44]. Structural studies showed the necessity of DCN1 in orienting the RING−E2−NEDD8 complex to a suitable conformation for NEDD8 transfer[41,43,101]. Human DCNL1 is found highly amplified in various tumors. It is reported that DCN1 mRNA is overexpressed in carcinomas of lung, prostate, head and neck, and cervix[102−106], appears to be essential for the transformation of squamous cell carcinoma (SCC)[54,107]. In addition, it appears that different DCNLs regulate different cullins in vivo[99,102]. This potential of cullin selectivity together with the important role in regulation of neddylation makes DCNLs intriguing targets for small-molecule inhibitors.

In 2010, Scott et al.[43] reported the duo-E3 mechanism by which DCN1 and RBX1/Hrt1 act together to promote neddylation in yeast, and demonstrated that the N-terminus of UBE2M was essential for DCN1−UBE2M interaction. The crystal structures later revealed that the first methionine residue of UBE2M was acetylated and buried in the hydrophobic pocket in DCN1[41], and that N-terminal acetylation of the E2s (both UBE2M and UBE2F) was a structurally conserved enhancer in the DCN1-dependent neddylation[41,42]. Furthermore, systematic biochemical assays showed that synthetic N-terminal peptides derived from UBE2M and UBE2F could compete with the full-length NEDD8 E2s, leading to potent inhibition of the DCN1-dependent in vitro neddylation reactions[41,42]. These findings not only defined an N-terminal acetylation-dependent mechanism in cullin neddylation, but also suggested the potential strategy of inhibiting cullin neddylation by disrupting the N-acetyl-methionine-dependent protein−protein interactions (PPIs).

3.2.1.   Piperidinyl urea-based inhibitors

In 2017, Scott et al.[108] reported the development of a series of piperidinyl urea targeting the N-terminal acetylation-dependent interaction between NEDD8 E2s and DCN1. Through a time-resolved fluorescence energy transfer (TR-FRET) based ligand competition assay, the authors screened more than 600,000 chemicals with SAR optimization and reported a chemical probe, designated as NAcM-HIT (Fig. 5A, #20). NAcM-HIT inhibited the DCN1-dependent neddylation reaction by specifically occupying the N-acetylmethionine-binding pocket (IC$_{50}$ = 4−7 μmol/L). Co-crystal structure of DCN1-NAcM-HIT (PDB: 5V83) revealed five sub-pockets in the DCN1−UBE2M binding site for ligand binding. Based on these pockets, together with a series of optimization studies, the authors further optimized and synthesized an analog (Fig. 5A, #21) with 100-fold increase in potency (IC$_{50}$ = 50−60 nmol/L). However, although this compound showed good solubility and permeability and significant DCN1 binding and on-target inhibitory effect in cells, it was rapidly metabolized in microsomal and murine models (clint = 165 mL/min/kg)[109]. This issue was further addressed through a set of rational structure-based design as well as empirical chemistry approaches, leading to the discovery of NAcM-OPT (Fig. 5A, #22, 5B), which is both potent (IC$_{50}$ = 60 nmol/L) and more stable in vitro and in vivo (clint = 25 mL/min/kg)[110]. NAcM-OPT showed selectivity towards DCN1−UBE2M interaction without affecting other acetyl-dependent protein interactions, and were specific for DCN1/2. Interestingly, in DCN1-highly-expressed squamous carcinoma cell line HCC95, NAcM-OPT inhibited neddylation of cullin-1 and -3, but not cullin-2, -4A and -5. Accordingly, NAcM-OPT caused a moderate accumulation of P27 and NRF2, the known substrate of cullin-1 and -3, respectively. But substrate of other cullins such as Cylin E or P21 was not affected. Overall, these were among the first class of small molecule inhibitors directly targeting E2−E3 protein−protein interaction in the neddylation cascade with selective inhibition of cullin neddylation via targeting DCN1[110].

3.2.2.   DI-591 and DI-404

Also in 2017, the Wang group[111] in collaboration with us independently discovered a distinct class of DCN1 inhibitor, designated as DI-591 (Fig. 5D, #23). DI-591 is a potent, specific and cell-permeable inhibitor targeting DCN1−UBE2M protein−protein interaction. Unlike the piperidinyl urea-based inhibitors, DI-591 was discovered through a structure-based design from the very beginning and incorporated with rigorous experimental design and extensive medicinal chemistry optimizations. Starting from a 12-residue peptide derived from the UBE2M N-terminus, the authors employed step-by-step structure-based optimization and eventually obtained the DI-591 with a K_i value of 12.4 nmol/L[111] and precisely binds to the sub-pockets in DCN1 (Fig. 5C and D). DI-591 has excellent aqueous solubility in both acidic and neutral conditions (>20 mmol/L[111] at pH 2.0 and 7.4).

Meanwhile, the Wang group[112] also discovered another high-affinity, peptidomimetic inhibitor of DCN1, designated as DI-404 (Fig. 5D, #24), through systematic optimizations targeting four important pockets in the DCN1−UBE2M interaction site. DI-404 potently binds to DCN1, with a K_d value of 6.7 nmol/L. Co-crystal structure further validated the high-affinity binding of DCN1 with DI-591 or DI-404, providing the structural insights into their mode of action. On cellular level, thermal shift assays demonstrated that DI-591 and DI-404 could specifically bind to
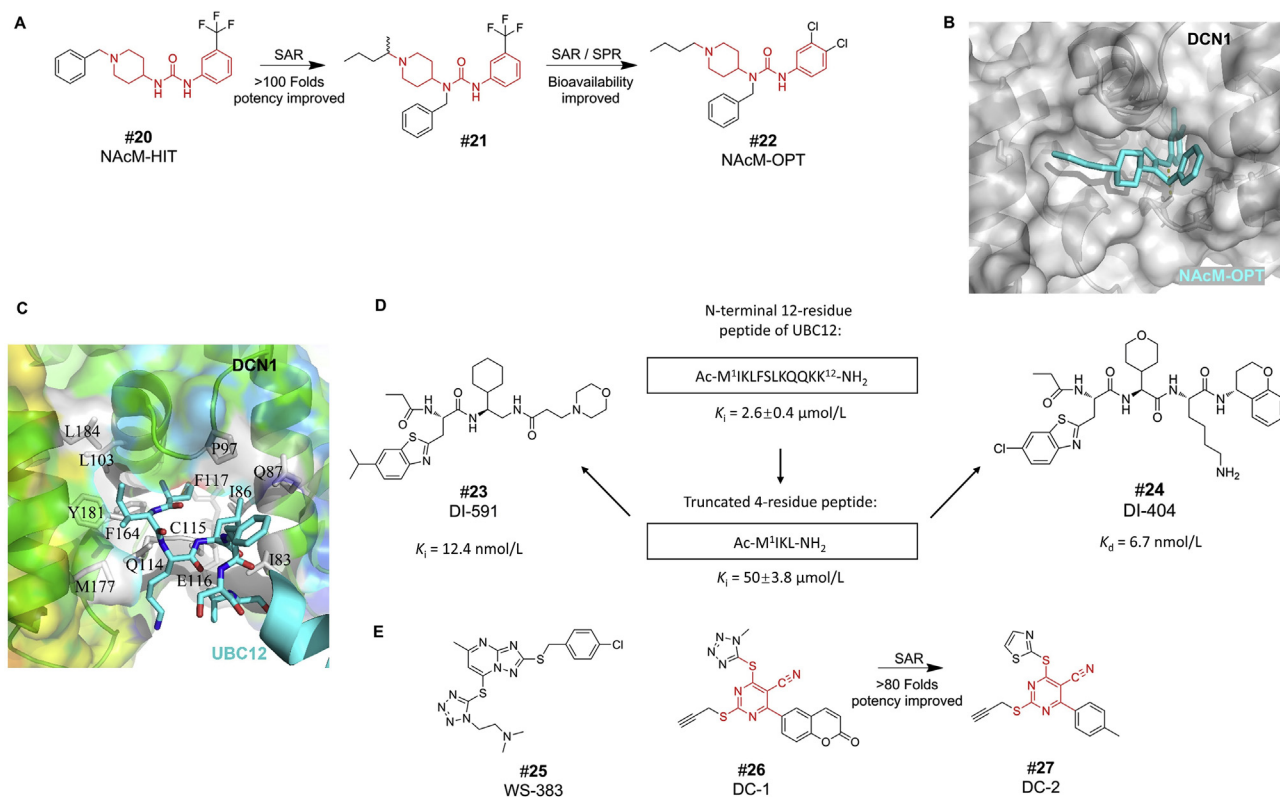
Figure 5 Chemical structures and the development of reported DCN-1 inhibitors. (A) The development of the piperidinyl urea-based DCN1 inhibitors; (B) the structure of NAcM-OPT docking into DCN1's pocket (PDB: 5VB6); (C) the co-crystal structure of DCN1 and the N-terminus of UBE2M (PDB: 3TDU); (D) the development of DI-591 and DI-404; (E) the structures of WS-383, DC-1 and DC-2.

DCN1. Consistently, co-immunoprecipitation (Co-IP) assays showed that DI-591 and DI-404 could block the association of DCN1 and UBE2M in cells. Interestingly, both DI-591 and DI-404 selectively inhibit neddylation of cullin-3 but not the other cullins. Accordingly, this selective inhibitory effect results in the effective accumulation of NRF2 protein, a substrate of cullin-3, but not the substrate of other cullins[111,112].

3.2.3. WS-383

A triazolo[1,5-a]pyrimidine-based DCN1 inhibitor, designated as WS-383, was recently reported by Shuai et al.[113] as another class of inhibitor specifically targeting DCN1−UBE2M interaction (Fig. 5E, #25). The compound was derived through the structure-based optimization of a candidate from the HRTF (homogeneous time resolved fluorescence)-based HTS. WS-383 had potent inhibitory activity *in vitro* ($IC_{50} = 11$ nmol/L). Molecular docking simulations showed that WS-383 docked into the hydrophobic binding pocket of DCN1. Besides, WS-383 possessed a heteroatom-tethered aromatic structure, which was shared by some small-molecule kinase inhibitors[114]. Enzyme assays showed that WS-383 only had weak inhibitory effect against a panel of kinases such as BTK, CDKs and EGFR [L858R], demonstrating WS-383 is a selective inhibitor of DCN1. Of note, the *in vitro* effect of WS-383 could be restored in a dilution assay as well as in an ultrafiltration experiment, indicating the WS-383/DCN1 binding was reversible. WS383 showed on-target engagement to DCN1 in gastric cell line MGC-803, and selectively inhibited neddylation of cullin-3 and -1, leading to accumulation of related

substrates such as NRF2, P21 and P27. These findings demonstrated that WS-383 is a potent and selective inhibitor targeting cellular DCN1−UBE2M interaction. However, WS-383 had poor pharmacodynamics which was rapidly metabolized with a high clearance rate in human, rat and dog liver microsomes[113].

3.2.4. DC-2

A most recent study by Zhou et al.[115] reported a new series of compounds that potently inhibit DCN1−UBE2M interaction. An FP and HTRF based screening using an in-house molecular library identified DC-1 (Fig. 5E, #26), as a specific DCN1 inhibitor ($IC_{50} = 1.2$ μmol/L). Extensive SAR efforts further yielded a series of derivatives with the 5-cyano-6-phenyl-pyrimidin scaffold and DC-2 (Fig. 5E, #27), the best candidate, exhibited the most potent inhibitory effect on DCN1−UBE2M interaction ($IC_{50} = 15$ nmol/L). Molecular docking and site-specific mutations further described the binding mode of DC-2 interacting with the binding pocket of DCN1. Cellular thermal shift assay (CETSA) showed that DC-2 indeed targets intracellular DCN1. Just like DI-591/DI-404, DC-2 specifically blocked cullin-3 neddylation in cells, leading to accumulation of NRF2 and the downstream proteins HO-1 and NQO1. Furthermore, DC-2 could effectively inhibit cell proliferation in a panel of DCN1-amplified cancer cells rather than two normal cell lines.

3.2.5. Perspectives for the DCN inhibitors

The discovery of several series of DCN1 inhibitors has significant impacts in the field of protein neddylation and its targeting by

small molecules. It shows the feasibility to target selective E2−E3 interaction in neddylation cascade. While the piperidinyl urea-based inhibitors selectively inhibited neddylation of cullin-3 and -1 over the other cullins, the series of DI-591/DI404 and DC-2 are highly selective in blocking cullin-3 neddylation without much effect on other cullins. The underlying mechanism for cullin-3 selectivity remains elusive at the present time. Nevertheless, the observation that NAcM-OPT strikingly decreased the association of UBC12/UBE2M with BTB proteins, the cullin-3 substrate receptors[108], may support the notion that cullin-3 is the most vulnerable target among all cullins. On the other hand, all current DCN1 inhibitors preferentially target DCN1/2 without affecting the DCN3-5, showing another level of selectivity. Finally, advantage of selective inhibition of cullin-3 neddylation is to avoid MLN4924-associated cytotoxicity due to targeting the entire neddylation pathway. Given NRF2, an antioxidant transcription factor, is a typical substrate of cullin-3[23], these series of selective compounds may have broad utility in the treatment of human diseases associated with over-production of reactive oxygen species (ROS).

3.3. A non-specific inhibitor of RBX1

A recent study reported that arsenite, an environment toxin, binds to the RING finger domain of RBX1 both *in vitro* and in cells[116]. Specifically, the *in vitro* binding assay showed an interaction between RING finger domain of RBX1 and arsenite. The cell based pull-down assay showed that biotin-labeled arsenite interacts with RBX1. Furthermore, by using As^{3+}-containing fluorescent dye (ReAsH), the authors showed a co-localization of the ectopically expressed RBX1 and ReAsH in HEK293T cells and identified RBX1-C83 as a key residue mediating the interaction *via* site-directed mutagenesis study. Finally, siRNA knockdown assay showed that arsenite binding to the RING finger domain of RBX1 is essential for inactivation of CRL-3 to cause NRF2 accumulation. However, no direct evidence was demonstrated that arsenite indeed inhibits cullin-3 neddylation. Furthermore, the binding specificity is a big issue, given the fact that arsenic is known to bind to many proteins, to inactivate up to 200 enzymes, including glutathione reductase, DNA ligases, Arg-tRNA protein transferase, pyruvate kinase galectin 1, protein tyrosine phosphatase, and a variety of RING E3 ligases[117]. Finally, mass spectrometry analysis revealed that arsenite interacts selectively with zinc finger motifs containing three or more cysteine residues (C3H1 or C4), but not that containing two cysteines (C2)[118], and RBX1 is a typical C3H2C3-containing RING finger protein[119]. Taken together, inactivation of RBX1 by arsenite is, therefore, rather non-specific.

4. Approaches to identify additional inhibitors of protein neddylation

4.1. Currently untapped targets

The neddylation process by E1/E2/E3 enzymatic cascade that transfers NEDD8 to a substrate involves multiple steps of the protein−protein interactions, including E1−E2, E2−E3s, E3−substrate, and NEDD8-target proteins. Each of these interactions is potential target for molecular modulation. The recent discovery of the DCN1 inhibitors provides an encouraging example of targeting the well-defined interaction pockets in the

DCN1−UBE2M interaction site. However, some PPI interface may lack such well-defined pocket, which makes it difficult to design selective and potent small-molecule inhibitors[120−122]. The enzymatic reactions for sequential transfer of NEDD8 to a substrate largely depend on PPIs, thus it is conceivable that the neddylation cascade may provide an overall target for the discovery of small-molecule inhibitors. Here we briefly summarize the current insight of structure-based interactions of E2s, RING E3s, and substrate to provide a general view for untapped targets in neddylation cascade. The structural, chemical and mechanistic details of each enzyme can be found in a comprehensive review recently published by Cappadocia and Lima[31].

4.1.1. E2s or E1−E2 interaction

Mammalian cells express one neddylation E1 (NEDD8-activating enzyme, NAE), a heterodimer, consisting of catalytic subunit UBA3/NAEβ, and regulatory subunit APPBP1/NAE1; and two E2s, UBC12/UBE2M and UBE2F. Both E2s bind NAE at two distinctive sites: the catalytic core domain of E2 interacts with UFD domain of UBA3, whereas and the N-terminal extension domain of the E2 binds to hydrophobic groove of UBA3[34,36,59,123]. Upon the formation of E1−NEDD8 thioester, the conformation changes of the UFD domain lead to the exposure of an E2 binding site. This binding mode is thought to be conserved across different UBLs cascades[34,59,124−128]. The N-terminal extension domain of UBE2M or UBE2F stabilizes and adopts an extended conformation within a groove on UBA3, which appears a unique feature that is only found in neddylation E1−E2 interaction[36,123]. This specificity provides a possibility for an NEDD8 E2 inhibitor to selectively target neddylation, but not the other UBLs modifications.

Moreover, the two NEDD8 E2s mediate different cullin neddylation. UBE2M couples through RBX1 to mediate neddylation of culllins 1−4, while UBE2F specifically works with RBX2 to neddylate cullin-5[36]. Although it is still unclear how NEDD8 E1 chooses between the two E2s, a possibility exists to selectively inhibit one of the two E2s to affect downstream cullin neddylation. For example, selective blockage of E1−UBE2F interaction would, in theory, inhibit cullin-5 neddylation only to causes accumulation of pro-apoptosis protein NOXA, a substrate of cullin-5, leading to apoptosis induction[129].

It is worth noting that CC0651, the first small-molecule inhibitor of ubiquitin E2 Cdc34, does not affect the E1−E2 or E2−E3 interactions[130]. Instead, CC0651 traps in a cryptic binding pocket on Cdc34 distant from the catalytic site, stabilizes the weak interaction between E2 and the donor ubiquitin, and slows down the discharge of ubiquitin to acceptor lysine residues[130,131]. CC0651 analogs caused P27 accumulation to inhibit cell proliferation in prostate and colorectal cancer cell lines. The CC0651 story suggested that allosteric inhibition is a feasible strategy for targeting E2 enzyme. More importantly, CC0651 showed remarkable selectivity for Cdc34 over the other E2 enzymes, which might be due to the sequence variation of the donor ubiquitin interaction surface across different E2s[131]. This interesting finding raised the possibility that CC0651 binding pocket might be a general allosteric modulating site that also exists in other E2s. A similar strategy could also be useful for designing specific inhibitors for neddylation E2s[130].

4.1.2. RING E3s or E2-RING E3 interaction

RBX1 and RBX2 are two E3 neddylation ligases that cooperate with E2 and DCN1, to promote neddylation of cullins, leading to

activation of Cullin−RING ligases (CRLs), which are responsible for ubiquitylation of ∼20% cellular proteins doomed for proteasomal degradation[26]. Structurally, the N-terminal domain of RBX1 is tethered to the C-terminal domain (CTD) of a substrate cullin, while the C-terminal RING domain of RBX1 recruits the UBE2M−NEDD8 intermediate[39]. Upon neddylation, RING domain stabilizes the UBE2M−NEDD8 in a closed, active conformation that poses the UBE2M−NEDD8 thioester bond for nucleophilic attack[101]. Thus, RBX1 adjoins the UBE2M−NEDD8 intermediate close to the bound substrate thereby facilitating the NEDD8 transfer to the substrate acceptor lysine residue[101]. A more detailed mechanism has been revealed recently by Schulman and colleagues with the co-crystal structure of RBX1−UBE2M−NEDD8−CUL1−DCN1, which shows how RBX1 specifically couples NEDD8 with cullin-1 in an NEDD8-target-dependent manner[101].

Although a handful of inhibitors have been reported to target the Cullin−RING Ubiquitin E3 ligases complex (e.g., thalidomide[132], SMER3[133], BC-1215[134], and ZL25[135]), those all target the non-RING subunits or block the protein−protein interaction between the E3 ligase and the substrate[136]. Few small molecules have been reported to inhibit MDM2 and POSH, two non-cullin RING E3s, but none of them shows direct binding to the RING finger scaffold[137,138]. Currently, no small-molecule inhibitor is reported that specifically and selectively targets the RING domain in E3s.

From a broader perspective, therapeutically targeting RING E3s are expected to have higher selectivity and less side effect, but it remains challenging for probing small molecules to the surface of RING E3s or E2−E3 interaction sites. Unlike NAE which harbors well-defined enzymatic activity pockets, RING E3s and the E2−E3 contact surfaces seemly lack such pockets or grooves or other structural features convenient for small molecule targeting[139].

4.1.3. Substrate-involved interactions

Cullin family proteins are the most-studied substrates of neddylation. Cullins bind to RING E3 (RBX1 or RBX2) with the C-terminal domain and are finally activated by the ligation of NEDD8 to a conserved lysine in the WHB subdomain in the CTD[140−142]. Among the eight members (CUL-1 to -3, -4a, -4b -5, -7 and -9/Parc)[17] of mammalian cullin proteins, CUL-1 and -5 are the only two with available cocrystal structures for a Cullin−RING−NEDD8 complex. NEDD8 is covalently attached to CUL-1 on Lys720 and CUL-5 on Lys724[37]. Structural studies have revealed that CUL-1 and -5 share some unique features that contribute to the efficient ligation of NEDD8. Specifically, the CUL-1 target site and UBE2M−NEDD8 linkage site are juxtaposed[101]. The complement interface ensures the effective ligation to NEDD8 to Lys720 on CUL-1, whereas deletion of two C-terminal residues of CUL-1 within the interface impaired neddylation[101]. Moreover, Try774 on CUL-1 was responsible for directing Lys720 into the active site to promote the NEDD8 ligation[101]. Similar observation was made in the crystal structure of NEDD8−CUL5^CTD−RBX1 in which the WHB domain within the CTD of cullin-5 contributed to effective NEDD8 ligation[37].

4.2. Approaches for identifying inhibitory compounds

The discovery of MLN4924, and subsequent preclinical and clinical studies provide solid evidence that targeting neddylation pathway is a feasible, effective and promising anticancer approach. However, the progress in targeting other neddylation enzymes is lagging. Unlike the druggable ATP-pocket in NAE, other targets in neddylation are largely based on PPIs, of which the contact surfaces are generally large, flat, and often exposed to solvent[143,144]. This nature of PPIs makes it really difficult to screen, design, or validate a specific PPI inhibitor[144]. What makes it even more challenging for targeting PPIs in neddylation process via structure-based drug design is the fact that it is a multi-component-containing, highly dynamic enzymatic cascade with diverse interaction surfaces and constantly changing conformations. Nevertheless, several approaches have been developed to screen for neddylation inhibitors and few selective UBLs inhibitors, as briefly summarized below.

4.2.1. Traditional HTS

Although in silico screening has become a leading trend in drug discovery, traditional high throughput screening still has its advantages in the case of exploring neddylation inhibitors. First, some neddylation enzymes lack for high-resolution crystal structures for structure-based drug design. Even with available structures, potential binding site may not be stable, since some interfaces undergo constant structural rearrangement during the neddylation cascade. For example, the inhibitors identified from a TR-FRET-based HTS were found to trap in a deep remodeled groove that normally accommodates the methionine side chain of UBE2M, whereas this deep groove was not observed in six prior structures of DCN family members in complex with the N-terminal acetylated NEDD8 E2s[108]. Nevertheless, a well-established biochemical assay designed for HTS makes it possible to replicate or mimic the dynamic interactions which might result in discovery of unexpected binding mode. Of note, most of the potent neddylation inhibitors discovered to date, including MLN4924, were initially identified in traditional HTS.

4.2.1.1. FRET/TR-FRET/HTRF

4.2.1.1.1. Assay principle.
Fluorescence resonance energy transfer (FRET) and time-resolved fluorescence resonance energy transfer (TR-FRET) are commonly used for establishing HTS format assays. In FRET/TR-FRET assays, a signal will be generated when a donor and an acceptor molecule reach close proximity, which causes fluorescent resonance energy transfer[145,146]. As an upgraded version of TR-FRET, homogeneous time resolved fluorescence (HTRF) combines FRET with time resolved measurement (TR) of fluorescence[147,148]. HTRF has several advantages over the traditional FRET including better assay flexibility, reliability and higher sensitivity[149].

4.2.1.1.2. Applications.
Detection of DCN1−UBE2M interaction: the piperidinyl urea DCN1 inhibitor was discovered via the HTS of a 600K library using a TR-FRET-based assay that generates specific signal between a biotinylated DCN1 protein, recognized by terbium-linked streptavidin, and a stapled peptide corresponding to N-terminally acetylated UBE2M labeled with a fluorescent dye AlexFluor 488 at its C-terminus[108,109]. The generated TR-FRET signal well represented the steady state of DCN1−UBE2M interaction.

In another study, Wang et al.[140] established an HTRF assay for the HTS of the DCN1−UBE2M inhibitors. The Eu^{3+}-cryptate conjugated GST antibody (donor beads) binds to the GST-DCN1 and the d2-conjugated streptavidin (accepter beads) for

recognizing N-terminal-acetyl UBE2M with C-terminal bio-tinylated. The assay was optimized for a 15K screening and yielded several candidates including WS-291 which was further developed into WS-383[140].

In vitro E1−E2 transthiolation assay: Soucy et al.[26] used this TR-FRET-based assay to measure the *in vitro* activity of NAE. An enzymatic reaction was carried out with a mixture containing UBE2M-GST, NEDD8-Flag, NAE, MgATP and glutathione in a proper buffer system, followed by incubation with Eu^{3+}-cryptate labeled Flag-M2-specific antibody and PHYCOLINK allophyco-cyanin-labeled GST-specific antibody. Signal was then detected using multimode readers.

In vitro K48 di-Ub assay: in an attempt to identify inhibitors of E3 ubiquitin ligases, Wu et al.[150] developed a FRET based *in vitro* assay that measures linkage-specific Ub−Ub transfer. They first prepared a donor Ub^{K48R} and a receptor Ub^{G75G76} that can only generate a single Ub−Ub isopeptide bond with specific K48 linkage. Either Ub carried a different fluorescent dye at designed position. By incubating this unique pair of Ubs with purified E1, Cdc34 E2 and $RBX1/CUL1^{CTD}$ E3 in an *in vitro* enzyme assay, a FRET signal is generated representing the formation of a stable di-Ub product. Application of this assay for HTS led to the discovery of a century-old drug suramin as an effective cullin−RING E3 inhibitor[150].

4.2.1.2. AlphaScreen

4.2.1.2.1. Assay principle.
Amplified luminescence proximity homogeneous assay screen (AlphaScreen®) is a bead-based system commonly used for detection of protein−protein interaction[151]. In a typical AlphaScreen assay, one protein is captured on the donor beads, and the other is captured on the acceptor beads. When two proteins interact, the donor bead is brought into close proximity of the acceptor bead to generate specific AlphaScreen signal. AlphaScreen usually yields particularly high signal and very low background, providing a large signal window. It's also easy for optimization.

4.2.1.2.2. Applications.
In vitro E1−E2 transthiolation assay: in the discovery of a small-molecule inhibitor of the Ub E1, an AlphaScreen assay was carried using the similar conditions as in the above TR-FRET E1−E2 transthiolation assay[152]. Briefly, the Biotin-tagged E2 and Flag-tagged NEDD8 were added to the established *in vitro* enzyme reaction containing E1. Streptavidin-coupled donor beads and anti-Flag-coupled acceptor beads were used for detection.

Detection of NAE−NEDD8 interaction: Zhong et al.[90] used the AlphaScreen assay for hit validation. A reaction was carried in a mixture containing His-NEDD8, GST-NAE, UBE2M, and MgATP. Glutathione-coated donor beads and Ni^{2+}-chelated acceptor beads were then added to generate AlphaScreen signal. The assay validated a Rhodium (III) complex as an NAE inhibitor.

4.2.2. Virtual screening and structure-based design
Docking, and structured-based virtual screening and drug design have become standard approaches for drug discovery when crystal structure of a target protein is available. Most NAE inhibitors discussed in previous sections were discovered through virtual screening methods, and summarized in Table 2. Below we briefly summarize what was learned from the discovery of current neddylation inhibitors through these approaches. Comprehensive and in-depth reviews on the advances and current limitations in virtual screening can be found in several recent articles[153−155].

4.2.2.1. Call for more complete co-crystal structures.
The fundamental basis for effective virtual screening or structure-based drug design is the high-resolution crystal structures of the target proteins and related protein complexes. In Table 3, we summarized the publically available X-ray or NMR structures of neddylation enzymes in PDB (www.pdb.org). Although high resolution structures for each enzyme had been largely resolved, it is highly in demand for more complete co-crystal structures for multi-component complexes with different poses at different stage of the neddylation cascade. For example, while most of the structures related to UBE2M E2 and RBX1 E3 are available, the co-crystal structure of RBX2 and its binding partners is still unsolved. RBX2 exclusively works with UBE2F to neddylate cullin-5[156], followed by ubiquitylation of a number of substrates, including pro-

Table 2 Approaches of structure-based virtual screening in the discovery of NAE inhibitors.

Compd.	Strategy	Structure (PDB ID)	Library size	Number of validated hit	Docking program	Library source	Ref.
#7 (LZ3)	Docking + pharmacophore modeling	3GZN	27,996	8	GOLD	Filtered ZINC library	84
#8 (6,6″-Biapigenin)	Docking	1R4N	20,000	NA	ICM-Pro	Natural product-like library	85
#9 (Deoxyvasicinone derivative)	Docking	1R4N	90,000	9	ICM-Pro	ZINC natural product database	86
#10, 11 (Deoxyvasicinone derivatives)	Pharmacophore modeling + ligand pharmacophore mapping	NA	376	NA	NA	In-house database	87
#15 (Piperacillin)	Docking	1R4N	>3000	4	ICM-Pro	FDA-proved drugs database	91
#16 (Mitoxantrone)	Docking	3GZN	>3000	9	ICM-Pro	FDA-proved drugs database	92
#17 (M22)	Docking	1R4N	50,000	23	LibDock, AutoDock	ChemBridge database	93
#19 (ZM223)	Docking	3GZN	150,000	9	Glide	Specs-Clean database	95

NA: not available.

Table 3 A list of X-ray or NMR structures of neddylation enzymes available in the PDB (www.rcsb.org)[a].

PDB ID (year)	Enzyme/ligand name	Method	Resolution
Single enzyme			
2KO3 (2009)	NEDD8	Solution NMR	−
1NDD (1999)	NEDD8	X-ray diffraction	1.6 Å
2LQ7 (2012)	E1	Solution NMR	−
1YOV (2005)	NAE (APPBP1/UBA3)	X-ray diffraction	2.6 Å
2EDI (2007)	UBE2F	Solution NMR	−
3O2U (2010)	UBE2M	X-ray diffraction	2.003 Å
2ECL (2007)	RBX2	Solution NMR	−
2LGV (2012)	RBX1	Solution NMR	−
3BQ3 (2008)	DCN1	X-ray diffraction	1.9 Å
Enzyme complex			
1R4N (2003)	APPBP1/UBA3/N8/ATP	X-ray diffraction	3.6 Å
3DBR (2008)	APPBP1/UBA3/N8	X-ray diffraction	3.05 Å
3DBL (2008)	APPBP1/UBA3/N8	X-ray diffraction	2.9 Å
3DBH (2008)	APPBP1/UBA3/N8	X-ray diffraction	2.85 Å
1R4M (2003)	APPBP1/UBA3/N8	X-ray diffraction	3 Å
2NVU (2007)	APPBP1/UBA3/UBE2M/N8/ATP	X-ray diffraction	2.8 Å
1TT5 (2004)	APPBP1/UBA3/UBE2M	X-ray diffraction	2.6 Å
3FN1 (2009)	UBA3/UBE2F	X-ray diffraction	2.5 Å
1Y8X (2004)	UBA3/UBE2M	X-ray diffraction	2.4 Å
3TDI (2011)	Dcnp1/UBE2M	X-ray diffraction	2.3 Å
4GBA (2012)	DCNL3/UBE2F	X-ray diffraction	2.4 Å
4GAO (2012)	DCNL2/UBE2M	X-ray diffraction	3.28 Å
3TDZ (2011)	DCNL1/CUL1/UBE2M	X-ray diffraction	2 Å
3TDU (2011)	DCNL1/CUL1/UBE2M	X-ray diffraction	1.5 Å
5V89 (2017)	DCN4-PONY/CUL1-WHB	X-ray diffraction	1.55 Å
3RTR (2011)	CUL1/RBX1	X-ray diffraction	3.21 Å
1LDJ (2002)	CUL1/RBX1	X-ray diffraction	3 Å
4P5O (2014)	CUL1/RBX1/DCNL1/UBE2M/NEDD8	X-ray diffraction	3.1071 Å
3DPL (2008)	CUL5/RBX1	X-ray diffraction	2.6 Å
3DQV (2008)	CUL5/RBX1/NEDD8	X-ray diffraction	3 Å
1U6G (2004)	CUL1/RBX1/CAND1	X-ray diffraction	3.1 Å
Enzyme(s)+small molecule inhibitor			
3GZN (2010)	APPBP1/UBA3/NEDD8/MLN4924	X-ray diffraction	3 Å
5UFI (2017)	DCN1/DI-591	X-ray diffraction	2.58 Å
6BG3 (2018)	DCN1/DOJ	X-ray diffraction	1.05 Å
6BG5 (2018)	DCN1/DQD	X-ray diffraction	1.1 Å
6B5Q (2018)	DCN1/DI591	X-ray diffraction	2.16 Å
5V83 (2017)	DCN1/NAcM-HIT	X-ray diffraction	2.002 Å
5V86 (2017)	DCN1/NAcM-OPT	X-ray diffraction	1.374 Å
5V88 (2017)	DCN1/NAcM-COV	X-ray diffraction	1.601 Å

− Not applicable.
[a]Structures deposited/available up to 18 June, 2019.

apoptosis protein NOXA[129]. Although RBX1 and RBX2 share the conserved RING domain, only 53% of overall sequence is identical[119]. The underlying mechanisms of how the E3s selectively pair with a cognate E2, and with respective cullin substrates remain unknown. Future efforts should be directed to resolve the structures of these unique pairs of E2−E3s and E3−cullins in order to identify highly selective inhibitors targeting these interactions.

4.2.2.2.   The art of structure-based design.   With the increasing number of crystal structures available for targeted enzymes, structure-based drug design has become an indispensable tool for chemical probe development, lead optimization, and as a complementary method for HTS and VS. The development of the DCN1 inhibitors by Zhou et al.[111] showed a perfect example of peptidomimetic-based drug design to target PPIs in neddylation

modification. Based on a covalent mapping analysis of the DCN1−UBE2M interaction sites, a 12-residue UBE2M peptide was first identified and synthesized as the shortest peptide with potent affinity to DCN1 (Ac-MIKLFSLKQQKK-NH$_2$, $K_i = 2.6$ μmol/L). Sequential removal of each amino acid from the 12-residue peptide resulted in a tetrapeptide (Ac-MIKL-NH$_2$) as the crucial yet shortest peptide for effective interaction. Starting from this tetrapeptide, extensive medicinal chemistry optimization was performed with constant evaluation of probe potency, selectivity and aqueous solubility, and finally leading to discovery of the potent, selective DCN1 inhibitors DI-591 and DI-404[111,112]. More examples can be found across the discoveries of the other neddylation inhibitors. The future drug discovery efforts will be no doubt the combination of all available approaches including traditional high-throughput screening, virtual screening, and

structure-based design, along with other innovative strategies, for a better rate of success.

4.2.3. Approaches for hits validation and lead compound declaration

The above screen-based techniques are established to identify candidate neddylation inhibitors. The follow-up validation and SAR optimization at the levels of biochemistry, cell biology and pharmacology in animals are essential preclinical studies for the discovery of lead compound for clinical trials. Here we summarized commonly used approaches from the HTS to validation and optimization of candidate neddylation inhibitors, leading to declare the lead compounds (Fig. 6).

4.2.3.1. Screen for PAINS or frequent hitters. With the development and continuous employment of high-throughput screenings in the drug discovery industry, a series of compounds are frequently identified in multiple HTS campaigns as active hits but finally excluded as false positives by orthogonal experiments. These compounds with specific structures were summarized by Baell and Holloway[157] in 2010 and designated as Pan Assay Interference Compounds (PAINS). The use of certain substructural filters to screen for PAINS or other frequent hitters (FH) has become common practice during the early stage of hits validation process after HTS campaigns. One of such filters can be accessed *via* online chemical modeling environment (OCHEM)[158], which is a free web-based platform with a collection of structural alerts to identify PAINS and FHs[159]. Recently, the new filters were developed specifically to identify FHs in AlphaScreen assays[160]. These filters are available at the OCHEM website (http://ochem.eu/alerts) and can be freely accessed with easy-to-use online tools. However, the concerns were raised
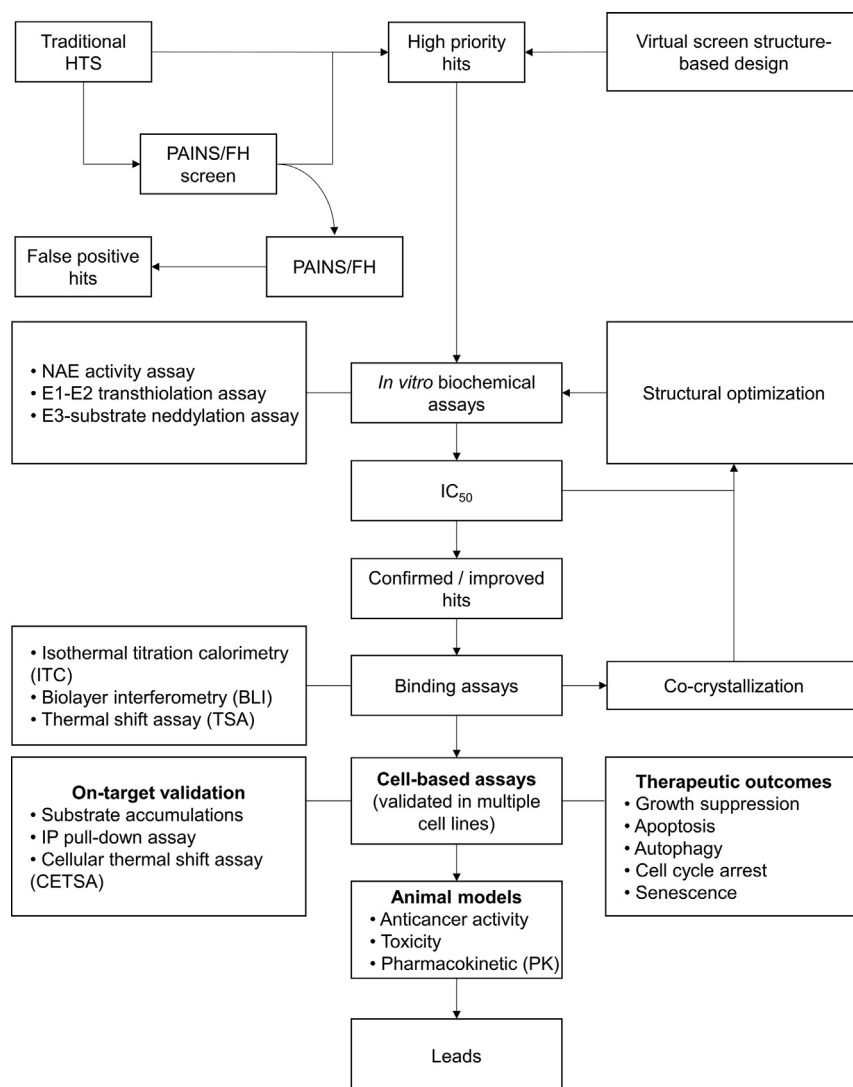

Figure 6 A flow chart for discovery of small molecule inhibitors of neddylation. The high priority hits that inhibit neddylation cascade can be obtained *via* either traditional HTS or virtual screen/structure-based design after the removal of potential false positive hits *via* PAINS/FH screens. These hits, along with their derivatives after SAR optimization, are evaluated *in vitro* by various biochemical assays for potency and selectivity. Optimized hits are then tested in cell-based assay for targeting binding, target modulation and further optimized *via* co-crystallization with targeted proteins. Cell-based biological assays are used to determine anti-cancer efficacy and nature of growth inhibition vial induction of apoptosis, autophagy, cell cycle arrest and senescence, followed by animal studies for *in vivo* anticancer activity, toxicity and pharmacokinetics. The best compound survived from these vigorous preclinical tests will then be the lead compound for clinical trials in human population.

recently that many of the PAINS or FHs filters may not be as informative as previously expected and should not be used as the sole exclusion of candidates[161]. Medicinal chemical optimization, and biochemical and cell-based assays are needed as more reliable approaches for candidate validation.

4.2.3.2.   Evaluation of binding affinities.   Candidate compounds identified *via* various screen methods are validated for potential binding with the targeting enzyme. Commonly, measurement of the binding affinity is performed through isothermal titration calorimetry (ITC)[73,109] or biolayer interferometry (BLI) method[112,115]. Alternatively, the thermal shift assay is also used to evaluate the *in vitro* binding of compounds and a purified target enzyme[115].

4.2.3.3.   Cell-based validation.   At the cellular levels, several approaches are commonly used to validate the candidate compounds. The first approach is to validate the target binding *via* various binding assays, including the biotinylated protein pull-down assay[108], co-immunoprecipitation assay, or cellular thermal shift assay (CETSA)[75,109,112,113,115]. The second approach is to validate the target modulation, such as inhibition of cullin neddylation, and accumulation of CRL substrates by Western blotting. Biological significance (*e.g.*, anticancer activity) can be evaluated *via* IC_{50}-based growth assays, and growth suppression evaluated by the assays for apoptosis, autophagy, senescence and cell arrest.

4.2.3.4.   Validation in animals.   The variety of *in vivo* xenograft tumor models are used to evaluate anticancer activity of compounds. The toxicity and pharmacokinetics assays are used to define maximum tolerable doses and the kinetics of compound decay in various animals.

A typical flow chart for discovery of small molecule inhibitors of neddylation is summarized in Fig. 6. Overall, the discovery of neddylation inhibitors, like discovery of any other drugs, is a lengthy process, which includes the HTS screening, candidate SAR optimization, *in vitro* and *in vivo* validation, *in vitro* and *in vivo* biological efficacy, and optimal toxicity and pharmacokinetics in animals before declaration of the best candidate, which meets rigorous criteria in each step, as the lead compound for clinical trial studies in human population.

5.   Conclusions and perspectives

In the past decade, we have witnessed a rapid progress in the field of protein neddylation. Studies in structural biology have revealed the underlying mechanism of the neddylation cascade at the molecular level. At the same time, our understanding of neddylation and its role in cancer biology has been largely extended by the broad applications and mechanism studies of the first-in-class inhibitor MLN4924 in multiple cancer cell lines, tumor xenografts models and a series of clinical trials. Following the discovery of MLN4924, a variety of drug discovery approaches have been undertaken to seek more selective and less toxic inhibitors targeting neddylation.

While MLN4924 remains the most effective neddylation inhibitor for cancer treatment, some highly selective neddylation inhibitors are emerging. The best example is the discovery of the DCN1 inhibitors which acts at the interaction between DCN1 and the acetylated N-terminus of UBE2M. Biological applications of these inhibitors are under the way with the main focus on the

diseases triggered by overproduction of ROS such as liver toxicity induced by acetaminophen overdosing (manuscript submitted), given their role in selective targeting CRL3 to cause accumulation of NRF2, an antioxidant transcription factor to scavenge ROS.

Besides NAE and the DCN1−UBE2M interaction site, other enzymes or PPIs in the neddylation cascades remain, however, largely untapped for specific small-molecule inhibitors. Future studies are directed to obtain more precise crystal or co-crystal structures with high resolution of UBE2F/UBE2M E2s, RBX1/2 RING E3s, and PPI interfaces involving E1−E2 or E2−RING E3, and E3−substrates alone or in combination of small molecules identified *via* various HTS. Structural based optimization and validation would eventually lead to discover and develop potent inhibitors targeting neddylation cascade for effective treatment of various human diseases, particularly cancer, with over-activated neddylation cascades.

Acknowledgment

Author contributions

Qing Yu wrote the first draft of the manuscript, Yihan Jiang made minor revisions and Yi Sun made major revisions and finalized the manuscript.

Conflicts of interest

The authors have no conflicts of interest to declare.

References

1. Hershko A. The ubiquitin system for protein degradation and some of its roles in the control of the cell division cycle. *Cell Death Differ* 2005;**12**:1191−7.
2. Hershko A, Ciechanover A. The ubiquitin system. *Annu Rev Biochem* 1998;**67**:425−79.
3. Varshavsky A. Regulated protein degradation. *Trends Biochem Sci* 2005;**30**:283−6.
4. Ye Y, Rape M. Building ubiquitin chains: E2 enzymes at work. *Nat Rev Mol Cell Biol* 2009;**10**:755−64.
5. Deshaies RJ, Joazeiro CAP. RING domain E3 ubiquitin ligases. *Annu Rev Biochem* 2009;**78**:399−434.
6. Schulman BA, Wade Harper J. Ubiquitin-like protein activation by E1 enzymes: the apex for downstream signalling pathways. *Nat Rev Mol Cell Biol* 2009;**10**:319−31.
7. Jin L, Williamson A, Banerjee S, Philipp I, Rape M. Mechanism of ubiquitin-chain formation by the human anaphase-promoting complex. *Cell* 2008;**133**:653−65.
8. Newton K, Matsumoto ML, Wertz IE, Kirkpatrick DS, Lill JR, Tan J, et al. Ubiquitin chain editing revealed by polyubiquitin linkage-specific antibodies. *Cell* 2008;**134**:668−78.
9. Walczak H, Iwai K, Dikic I. Generation and physiological roles of linear ubiquitin chains. *BMC Biol* 2012;**10**:23.
10. Wickliffe KE, Williamson A, Meyer HJ, Kelly A, Rape M. K11-linked ubiquitin chains as novel regulators of cell division. *Trends Cell Biol* 2011;**21**:656−63.
11. Popovic D, Vucic D, Dikic I. Ubiquitination in disease pathogenesis and treatment. *Nat Med* 2014;**20**:1242−53.
12. Imajoh-Ohmi S, Kawaguchi T, Sugiyama S, Tanaka K, Omura S, Kikuchi H. Lactacystin, a specific inhibitor of the proteasome,

induces apoptosis in human monoblast U937 cells. *Biochem Biophys Res Commun* 1995;**217**:1070−7.

13. Shinohara K, Tomioka M, Nakano H, Toné S, Ito H, Kawashima S. Apoptosis induction resulting from proteasome inhibition. *Biochem J* 1996;**317**:385−8.

14. Kane RC, Dagher R, Farrell A, Ko CW, Sridhara R, Justice R, et al. Bortezomib for the treatment of mantle cell lymphoma. *Clin Cancer Res* 2007;**13**:5291−4.

15. Richardson PG, Barlogie B, Berenson J, Singhal S, Jagannath S, Irwin D, et al. A phase 2 study of bortezomib in relapsed, refractory myeloma. *N Engl J Med* 2003;**348**:2609−17.

16. Enchev RI, Schulman BA, Peter M. Protein neddylation: beyond cullin−RING ligases. *Nat Rev Mol Cell Biol* 2015;**16**:30−44.

17. Sarikas A, Hartmann T, Pan ZQ. The cullin protein family. *Genome Biol* 2011;**12**:220.

18. Li C, Du L, Ren Y, Liu X, Jiao Q, Cui D, et al. SKP2 promotes breast cancer tumorigenesis and radiation tolerance through PDCD4 ubiquitination. *J Exp Clin Cancer Res* 2019;**38**:76.

19. Yada M, Hatakeyama S, Kamura T, Nishiyama M, Tsunematsu R, Imaki H, et al. Phosphorylation-dependent degradation of c-Myc is mediated by the F-box protein Fbw7. *EMBO J* 2004;**23**:2116−25.

20. Wan M, Tang Y, Tytler EM, Lu C, Jin B, Vickers SM, et al. Smad4 protein stability is regulated by ubiquitin ligase SCF$^{\beta\text{-TrCP1}}$. *J Biol Chem* 2004;**279**:14484−7.

21. Abida WM, Nikolaev A, Zhao W, Zhang W, Gu W. FBXO11 promotes the neddylation of P53 and inhibits its transcriptional activity. *J Biol Chem* 2007;**282**:1797−804.

22. Soucy TA, Dick LR, Smith PG, Milhollen MA, Brownell JE. The NEDD8 conjugation pathway and its relevance in cancer biology and therapy. *Genes Cancer* 2010;**1**:708−16.

23. Zhao Y, Morgan MA, Sun Y. Targeting neddylation pathways to inactivate cullin−RING ligases for anticancer therapy. *Antioxid Redox Signal* 2014;**21**:2383−400.

24. Zhou L, Zhang W, Sun Y, Jia L. Protein neddylation and its alterations in human cancers for targeted therapy. *Cell Signal* 2018;**44**:92−102.

25. Tanaka T, Nakatani T, Kamitani T. Inhibition of NEDD8-conjugation pathway by novel molecules: potential approaches to anticancer therapy. *Mol Oncol* 2012;**6**:267−75.

26. Soucy TA, Smith PG, Milhollen MA, Berger AJ, Gavin JM, Adhikari S, et al. An inhibitor of NEDD8-activating enzyme as a new approach to treat cancer. *Nature* 2009;**458**:732−6.

27. Soucy TA, Smith PG, Rolfe M. Targeting NEDD8-activated cullin−RING ligases for the treatment of cancer. *Clin Cancer Res* 2009;**15**:3912−6.

28. Van Der Veen AG, Ploegh HL. Ubiquitin-like proteins. *Annu Rev Biochem* 2012;**81**:323−57.

29. Whitby FG, Xia G, Pickart CM, Hill CP. Crystal structure of the human ubiquitin-like protein NEDD8 and interactions with ubiquitin pathway enzymes. *J Biol Chem* 1998;**273**:34983−91.

30. Walden H, Podgorski MS, Huang DT, Miller DW, Howard RJ, Minor DL, et al. The structure of the APPBP1−UBA3−NEDD8−ATP complex reveals the basis for selective ubiquitin-like protein activation by an E1. *Mol Cell* 2003;**12**:1427−37.

31. Cappadocia L, Lima CD. Ubiquitin-like protein conjugation: structures, chemistry, and mechanism. *Chem Rev* 2018;**118**:889−918.

32. Gong L, Yeh ET. Identification of the activating and conjugating enzymes of the NEDD8 conjugation pathway. *J Biol Chem* 1999;**274**:12036−42.

33. Bohnsack RN, Haas AL. Conservation in the mechanism of Nedd8 activation by the human AppBp1−Uba3 heterodimer. *J Biol Chem* 2003;**278**:26823−30.

34. Huang DT, Hunt HW, Zhuang M, Ohi MD, Holton JM, Schulman BA. Basis for a ubiquitin-like protein thioester switch toggling E1−E2 affinity. *Nature* 2007;**445**:394−8.

35. Liakopoulos D, Doenges G, Matuschewski K, Jentsch S. A novel protein modification pathway related to the ubiquitin system. *EMBO J* 1998;**17**:2208−14.

36. Huang DT, Ayrault O, Hunt HW, Taherbhoy AM, Duda DM, Scott DC, et al. E2−RING expansion of the NEDD8 cascade confers specificity to cullin modification. *Mol Cell* 2009;**33**:483−95.

37. Duda DM, Borg LA, Scott DC, Hunt HW, Hammel M, Schulman BA. Structural insights into NEDD8 activation of cullin−RING ligases: conformational control of conjugation. *Cell* 2008;**134**:995−1006.

38. Zheng N, Wang P, Jeffrey PD, Pavletich NP. Structure of a c-Cbl−UbcH7 complex: RING domain function in ubiquitin−protein ligases. *Cell* 2000;**102**:533−9.

39. Zheng N, Schulman BA, Song L, Miller JJ, Jeffrey PD, Wang P, et al. Structure of the Cul1−Rbx1−Skp1−F box^{Skp2} SCF ubiquitin ligase complex. *Nature* 2002;**416**:703−9.

40. Kurz T, Ozlü N, Rudolf F, O'Rourke SM, Luke B, Hofmann K, et al. The conserved protein DCN-1/Dcn1p is required for cullin neddylation in *C. elegans* and *S. cerevisiae*. *Nature* 2005;**435**:1257−61.

41. Scott DC, Monda JK, Bennett EJ, Harper JW, Schulman BA. N-terminal acetylation acts as an avidity enhancer within an interconnected multiprotein complex. *Science* 2011;**334**:674−8.

42. Monda JK, Scott DC, Miller DJ, Lydeard J, King D, Harper JW, et al. Structural conservation of distinctive N-terminal acetylation-dependent interactions across a family of mammalian NEDD8 ligation enzymes. *Structure* 2013;**21**:42−53.

43. Scott DC, Monda JK, Grace CR, Duda DM, Kriwacki RW, Kurz T, et al. A dual E3 mechanism for Rub1 ligation to Cdc53. *Mol Cell* 2010;**39**:784−96.

44. Kurz T, Chou YC, Willems AR, Meyer-Schaller N, Hecht ML, Tyers M, et al. Dcn1 functions as a scaffold-type E3 ligase for cullin neddylation. *Mol Cell* 2008;**29**:23−35.

45. Mo Z, Zhang Q, Liu Z, Lauer J, Shi Y, Sun L, et al. Neddylation requires glycyl-tRNA synthetase to protect activated E2. *Nat Struct Mol Biol* 2016;**23**:730−7.

46. Rabut G, Le Dez G, Verma R, Makhnevych T, Knebel A, Kurz T, et al. The TFIIH subunit Tfb3 regulates cullin neddylation. *Mol Cell* 2011;**43**:488−95.

47. Zhou W, Xu J, Tan M, Li H, Li H, Wei W, et al. UBE2M is a stress-inducible dual E2 for neddylation and ubiquitylation that promotes targeted degradation of UBE2F. *Mol Cell* 2018;**70**:1008−1024.e6.

48. Jia L, Soengas MS, Sun Y. ROC1/RBX1 E3 ubiquitin ligase silencing suppresses tumor cell growth *via* sequential induction of G₂−M arrest, apoptosis, and senescence. *Cancer Res* 2009;**69**:4974−82.

49. Gao Q, Yu GY, Shi JY, Li LH, Zhang WJ, Wang ZC, et al. Neddylation pathway is up-regulated in human intrahepatic cholangiocarcinoma and serves as a potential therapeutic target. *Oncotarget* 2014;**5**:7820−32.

50. Xie P, Zhang M, He S, Lu K, Chen Y, Xing G, et al. The covalent modifier Nedd8 is critical for the activation of Smurf1 ubiquitin ligase in tumorigenesis. *Nat Commun* 2014;**5**:3733.

51. Chen P, Hu T, Liang Y, Li P, Chen X, Zhang J, et al. Neddylation inhibition activates the extrinsic apoptosis pathway through ATF4−CHOP−DR5 axis in human esophageal cancer cells. *Clin Cancer Res* 2016;**22**:4145−57.

52. Hua W, Li C, Yang Z, Li L, Jiang Y, Yu G, et al. Suppression of glioblastoma by targeting the overactivated protein neddylation pathway. *Neuro Oncol* 2015;**17**:1333−43.

53. Barbier-Torres L, Delgado TC, García-Rodríguez JL, Zubiete-Franco I, Fernández-Ramos D, Buqué X, et al. Stabilization of LKB1 and Akt by neddylation regulates energy metabolism in liver cancer. *Oncotarget* 2015;**6**:2509−23.

54. Sarkaria I, O-Charoenrat P, Talbot SG, Reddy PG, Ngai I, Maghami E, et al. Squamous cell carcinoma related oncogene/*DCUN1D1* is highly conserved and activated by amplification in squamous cell carcinomas. *Cancer Res* 2006;**66**:9437−44.

55. Xie P, Yang JP, Cao Y, Peng LX, Zheng LS, Sun R, et al. Promoting tumorigenesis in nasopharyngeal carcinoma, NEDD8 serves as a potential theranostic target. *Cell Death Dis* 2017;**8**:e2834.

56. Li L, Wang M, Yu G, Chen P, Li H, Wei D, et al. Overactivated neddylation pathway as a therapeutic target in lung cancer. *J Natl Cancer Inst* 2014;**106**:dju083.

57. Olsen SK, Lima CD. Structure of a ubiquitin E1−E2 complex: insights to E1−E2 thioester transfer. *Mol Cell* 2013;**49**:884−96.

58. Tokgöz Z, Siepmann TJ, Streich Jr F, Kumar B, Klein JM, Haas AL. E1−E2 interactions in ubiquitin and Nedd8 ligation pathways. *J Biol Chem* 2012;**287**:311−21.

59. Huang DT, Paydar A, Zhuang M, Waddell MB, Holton JM, Schulman BA. Structural basis for recruitment of Ubc12 by an E2 binding domain in NEDD8's E1. *Mol Cell* 2005;**17**:341−50.

60. Wu P, Nielsen TE, Clausen MH. FDA-approved small-molecule kinase inhibitors. *Trends Pharmacol Sci* 2015;**36**:422−39.

61. Brownell JE, Sintchak MD, Gavin JM, Liao H, Bruzzese FJ, Bump NJ, et al. Substrate-assisted inhibition of ubiquitin-like protein-activating enzymes: the NEDD8 E1 inhibitor MLN4924 forms a NEDD8-AMP mimetic in situ. *Mol Cell* 2010;**37**:102−11.

62. Lux MC, Standke LC, Tan DS. Targeting adenylate-forming enzymes with designed sulfonyladenosine inhibitors. *J Antibiot (Tokyo)* 2019;**72**:325−49.

63. Yang Y, Kitagaki J, Dai RM, Tsai YC, Lorick KL, Ludwig RL, et al. Inhibitors of ubiquitin-activating enzyme (E1), a new class of potential cancer therapeutics. *Cancer Res* 2007;**67**:9472−81.

64. Bhatia S, Pavlick AC, Boasberg P, Thompson JA, Mulligan G, Pickard MD, et al. A phase I study of the investigational NEDD8-activating enzyme inhibitor pevonedistat (TAK-924/MLN4924) in patients with metastatic melanoma. *Invest New Drugs* 2016;**34**: 439−49.

65. Swords RT, Erba HP, DeAngelo DJ, Bixby DL, Altman JK, Maris M, et al. Pevonedistat (MLN4924), a first-in-class NEDD8-activating enzyme inhibitor, in patients with acute myeloid leukaemia and myelodysplastic syndromes: a phase 1 study. *Br J Haematol* 2015; **169**:534−43.

66. Sarantopoulos J, Shapiro GI, Cohen RB, Clark JW, Kauh JS, Weiss GJ, et al. Phase I study of the investigational NEDD8-activating enzyme inhibitor pevonedistat (TAK-924/MLN4924) in patients with advanced solid tumors. *Clin Cancer Res* 2016;**22**: 847−57.

67. Shah JJ, Jakubowiak AJ, O'Connor OA, Orlowski RZ, Harvey RD, Smith MR, et al. Phase I study of the novel investigational NEDD8-activating enzyme inhibitor pevonedistat (MLN4924) in patients with relapsed/refractory multiple myeloma or lymphoma. *Clin Cancer Res* 2016;**22**:34−43.

68. Nawrocki ST, Griffin P, Kelly KR, Carew JS. MLN4924: a novel first-in-class inhibitor of NEDD8-activating enzyme for cancer therapy. *Expert Opin Investig Drugs* 2012;**21**:1563−73.

69. Brown P, Richardson CM, Mensah LM, O'Hanlon PJ, Osborne NF, Pope AJ, et al. Molecular recognition of tyrosinyl adenylate analogues by prokaryotic tyrosyl tRNA synthetases. *Bioorg Med Chem* 1999;**7**:2473−85.

70. Wilkinson KD, Smith SE, O'Connor L, Sternberg E, Taggart JJ, Berges DA, et al. A specific inhibitor of the ubiquitin activating enzyme: synthesis and characterization of adenosyl-phospho-ubiquitinol, a nonhydrolyzable ubiquitin adenylate analog. *Biochemistry* 1990;**29**:7373−80.

71. Zhou L, Jiang Y, Luo Q, Li L, Jia L. Neddylation: a novel modulator of the tumor microenvironment. *Mol Cancer* 2019;**18**:77.

72. Zhou Q, Li H, Li Y, Tan M, Fan S, Cao C, et al. Inhibiting neddylation modification alters mitochondrial morphology and reprograms energy metabolism in cancer cells. *JCI Insight* 2019;**4**:e121582.

73. Chen JJ, Tsu CA, Gavin JM, Milhollen MA, Bruzzese FJ, Mallender WD, et al. Mechanistic studies of substrate-assisted inhibition of ubiquitin-activating enzyme by adenosine sulfamate analogues. *J Biol Chem* 2011;**286**:40867−77.

74. Lukkarila JL, Da Silva SR, Ali M, Shahani VM, Xu GW, Berman J, et al. Identification of NAE inhibitors exhibiting potent activity in

75. leukemia cells: exploring the structural determinants of NAE specificity. *ACS Med Chem Lett* 2011;**2**:577−82.

76. Zhou X, Tan M, Nyati MK, Zhao Y, Wang G, Sun Y. Blockage of neddylation modification stimulates tumor sphere formation *in vitro* and stem cell differentiation and wound healing *in vivo*. *Proc Natl Acad Sci U S A* 2016;**113**:E2935−44.

77. Mao H, Tang Z, Li H, Sun B, Tan M, Fan S, et al. Neddylation inhibitor MLN4924 suppresses cilia formation by modulating AKT1. *Protein Cell* 2019;**10**:726−44.

78. Yoshimura C, Muraoka H, Ochiiwa H, Tsuji S, Hashimoto A, Kazuno H, et al. TAS4464, a highly potent and selective inhibitor of NEDD8-activating enzyme, suppresses neddylation and shows antitumor activity in diverse cancer models. *Mol Cancer Ther* 2019;**18**: 1205−16.

79. Nishitani H, Sugimoto N, Roukos V, Nakanishi Y, Saijo M, Obuse C, et al. Two E3 ubiquitin ligases, SCF-Skp2 and DDB1-Cul4, target human Cdt1 for proteolysis. *EMBO J* 2006;**25**:1126−36.

80. Kobayashi A, Kang MI, Okawa H, Ohtsuji M, Zenke Y, Chiba T, et al. Oxidative stress sensor Keap1 functions as an adaptor for Cul3-based E3 ligase to regulate proteasomal degradation of Nrf2. *Mol Cell Biol* 2004;**24**:7130−9.

81. Read MA, Brownell JE, Gladysheva TB, Hottelet M, Parent LA, Coggins MB, et al. Nedd8 modification of CUL-1 activates SCFβ^{TrCP}-dependent ubiquitination of I$\kappa B\alpha$. *Mol Cell Biol* 2000;**20**: 2326−33.

82. Carrano AC, Eytan E, Hershko A, Pagano M. SKP2 is required for ubiquitin-mediated degradation of the CDK inhibitor P27. *Nat Cell Biol* 1999;**1**:193−9.

83. An H, Statsyuk AV. Development of activity-based probes for ubiquitin and ubiquitin-like protein signaling pathways. *J Am Chem Soc* 2013;**135**:16948−62.

84. An H, Statsyuk AV. An inhibitor of ubiquitin conjugation and aggresome formation. *Chem Sci* 2015;**6**:5235−45.

85. Zhang S, Tan J, Lai Z, Li Y, Pang J, Xiao J, et al. Effective virtual screening strategy toward covalent ligands: identification of novel NEDD8-activating enzyme inhibitors. *J Chem Inf Model* 2014;**54**: 1785−97.

86. Leung CH, Chan DS, Yang H, Abagyan R, Lee SM, Zhu GY, et al. A natural product-like inhibitor of NEDD8-activating enzyme. *Chem Commun* 2011;**47**:2511−3.

87. Zhong HJ, Ma VP, Cheng Z, Chan DS, He HZ, Leung KH, et al. Discovery of a natural product inhibitor targeting protein neddylation by structure-based virtual screening. *Biochimie* 2012;**94**:2457−60.

88. Zhong HJ, Leung KH, Lin S, Chan DS, Han QB, Chan SL, et al. Discovery of deoxyvasicinone derivatives as inhibitors of NEDD8-activating enzyme. *Methods* 2015;**71**:71−6.

89. Li X, Yokoyama NN, Zhang S, Ding L, Liu HM, Lilly MB, et al. Flavokawain A induces deNEDDylation and Skp2 degradation leading to inhibition of tumorigenesis and cancer progression in the TRAMP transgenic mouse model. *Oncotarget* 2015;**6**:41809−24.

90. Zhong HJ, Yang H, Chan DS, Leung CH, Wang HM, Ma DL. A metal-based inhibitor of NEDD8-activating enzyme. *PLoS One* 2012; **7**:e49574.

91. Zhong HJ, Wang W, Kang TS, Yan H, Yang Y, Xu L, et al. A rhodium(III) complex as an inhibitor of neural precursor cell expressed, developmentally down-regulated 8-activating enzyme with *in vivo* activity against inflammatory bowel disease. *J Med Chem* 2017;**60**: 497−503.

92. Zhong HJ, Liu LJ, Chan DS, Wang HM, Chan PW, Ma DL, et al. Structure-based repurposing of FDA-approved drugs as inhibitors of NEDD8-activating enzyme. *Biochimie* 2014;**102**:211−5.

93. Wu KJ, Zhong HJ, Li G, Liu C, Wang HM, Ma DL, et al. Structure-based identification of a NEDD8-activating enzyme inhibitor *via* drug repurposing. *Eur J Med Chem* 2018;**143**:1021−7.

94. Lu P, Liu X, Yuan X, He M, Wang Y, Zhang Q, et al. Discovery of a novel NEDD8 activating enzyme inhibitor with piperidin-4-amine

scaffold by structure-based virtual screening. *ACS Chem Biol* 2016;
11:1901−7.

94. Lu P, Guo Y, Zhu L, Xia Y, Zhong Y, Wang Y. A novel NAE/UAE
dual inhibitor LP0040 blocks neddylation and ubiquitination leading
to growth inhibition and apoptosis of cancer cells. *Eur J Med Chem*
2018;**154**:294−304.

95. Ma H, Zhuang C, Xu X, Li J, Wang J, Min X, et al. Discovery of
benzothiazole derivatives as novel non-sulfamide NEDD8 activating
enzyme inhibitors by target-based virtual screening. *Eur J Med Chem*
2017;**133**:174−83.

96. Critchley S, Gant TG, Langston SP, Olhava EJ, Peluso S. *Inhibitors
of E1 activating enzymes*. 2006. WO2006084281.

97. Bommeljé CC, Weeda VB, Huang G, Shah K, Bains S, Buss E, et al.
Oncogenic function of SCCRO5/DCUN1D5 requires its neddylation
E3 activity and nuclear localization. *Clin Cancer Res* 2014;**20**:
372−81.

98. Kim AY, Bommeljé CC, Lee BE, Yonekawa Y, Choi L, Morris LG,
et al. SCCRO (DCUN1D1) is an essential component of the E3
complex for neddylation. *J Biol Chem* 2008;**283**:33211−20.

99. Meyer-Schaller N, Chou YC, Sumara I, Martin DD, Kurz T,
Katheder N, et al. The human Dcn1-like protein DCNL3 promotes
Cul3 neddylation at membranes. *Proc Natl Acad Sci U S A* 2009;**106**:
12365−70.

100. Huang G, Stock C, Bommeljé CC, Weeda VB, Shah K, Bains S, et al.
SCCRO3 (DCUN1D3) antagonizes the neddylation and oncogenic
activity of SCCRO (DCUN1D1). *J Biol Chem* 2014;**289**:34728−42.

101. Scott DC, Sviderskiy VO, Monda JK, Lydeard JR, Cho SE,
Harper JW, et al. Structure of a RING E3 trapped in action reveals
ligation mechanism for the ubiquitin-like protein NEDD8. *Cell* 2014;
157:1671−84.

102. Wu K, Yan H, Fang L, Wang X, Pfleger C, Jiang X, et al. Mono-
ubiquitination drives nuclear export of the human DCN1-like protein
hDCNL1. *J Biol Chem* 2011;**286**:34060−70.

103. Petersen I, Bujard M, Petersen S, Wolf G, Goeze A, Schwendel A,
et al. Patterns of chromosomal imbalances in adenocarcinoma
and squamous cell carcinoma of the lung. *Cancer Res* 1997;**57**:
2331−5.

104. Heselmeyer K, Macville M, Schröck E, Blegen H, Hellström AC,
Shah K, et al. Advanced-stage cervical carcinomas are defined by a
recurrent pattern of chromosomal aberrations revealing high genetic
instability and a consistent gain of chromosome arm 3q. *Genes
Chromosomes Cancer* 1997;**19**:233−40.

105. Singh B, Stoffel A, Gogineni S, Poluri A, Pfister DG, Shaha AR,
et al. Amplification of the 3q26.3 locus is associated with progression
to invasive cancer and is a negative prognostic factor in head and
neck squamous cell carcinomas. *Am J Pathol* 2002;**161**:365−71.

106. Zhang ZH, Li J, Luo F, Wang YS. Clinical significance of SCCRO
(DCUN1D1) in prostate cancer and its proliferation-inhibiting effect
on Lncap cells. *Eur Rev Med Pharmacol Sci* 2017;**21**:4283−91.

107. Broderick SR, Golas BJ, Pham D, Towe CW, Talbot SG, Kaufman A,
et al. *SCCRO* promotes glioma formation and malignant progression
in mice. *Neoplasia* 2010;**12**:476−84.

108. Scott DC, Hammill JT, Min J, Rhee DY, Connelly M, Sviderskiy VO,
et al. Blocking an N-terminal acetylation-dependent protein inter-
action inhibits an E3 ligase. *Nat Chem Biol* 2017;**13**:850−7.

109. Hammill JT, Scott DC, Min J, Connelly MC, Holbrook G, Zhu F,
et al. Piperidinyl ureas chemically control defective in cullin ned-
dylation 1 (DCN1)-mediated cullin neddylation. *J Med Chem* 2018;
61:2680−701.

110. Hammill JT, Bhasin D, Scott DC, Min J, Chen Y, Lu Y, et al. Dis-
covery of an orally bioavailable inhibitor of defective in cullin
neddylation 1 (DCN1)-mediated cullin neddylation. *J Med Chem*
2018;**1**:2694−706.

111. Zhou H, Lu J, Liu L, Bernard D, Yang CY, Fernandez-Salas E, et al.
A potent small-molecule inhibitor of the DCN1−UBC12 interaction
that selectively blocks cullin 3 neddylation. *Nat Commun* 2017;**8**:
1150.

112. Zhou H, Zhou W, Zhou B, Liu L, Chern TR, Chinnaswamy K, et al.
High-affinity peptidomimetic inhibitors of the DCN1−UBC12
protein−protein interaction. *J Med Chem* 2018;**61**:1934−50.

113. Wang S, Zhao L, Shi XJ, Ding L, Yang L, Wang ZZ, et al. Devel-
opment of highly potent, selective, and cellular active triazolo[1,5-*a*]
pyrimidine-based inhibitors targeting the DCN1−UBC12
protein−protein interaction. *J Med Chem* 2019;**62**:2772−97.

114. Wu P, Nielsen TE, Clausen MH. Small-molecule kinase inhibitors:
an analysis of FDA-approved drugs. *Drug Discov Today* 2016;**21**:
5−10.

115. Zhou W, Ma L, Ding L, Guo Q, He Z, Yang J, et al. Potent 5-cyano-
6-phenyl-pyrimidin-based derivatives targeting DCN1−UBE2M
interaction. *J Med Chem* 2019;**62**:5382−403.

116. Jiang J, Tam LM, Wang P, Wang Y. Arsenite targets the RING finger
domain of Rbx1 E3 ubiquitin ligase to inhibit proteasome-mediated
degradation of Nrf2. *Chem Res Toxicol* 2018;**31**:380−7.

117. Shen S, Li XF, Cullen WR, Weinfeld M, Le XC. Arsenic binding to
proteins. *Chem Rev* 2013;**113**:7769−92.

118. Zhou X, Sun X, Cooper KL, Wang F, Liu KJ, Hudson LG. Arsenite
interacts selectively with zinc finger proteins containing C3H1 or C4
motifs. *J Biol Chem* 2011;**286**:22855−63.

119. Sun Y, Tan M, Duan H, Swaroop M. *SAG/ROC/Rbx/Hrt*, a zinc RING
finger gene family: molecular cloning, biochemical properties, and
biological functions. *Antioxid Redox Signal* 2001;**3**:635−50.

120. Chène P. Drugs targeting protein−protein interactions. *Chem-
MedChem* 2006;**1**:400−11.

121. Whitty A, Kumaravel G. Between a rock and a hard place?. *Nat
Chem Biol* 2006;**2**:112−8.

122. Fry DC. Drug-like inhibitors of protein−protein interactions: a
structural examination of effective protein mimicry. *Curr Protein
Pept Sci* 2008;**9**:240−7.

123. Huang DT, Miller DW, Mathew R, Cassell R, Holton JM,
Roussel MF, et al. A unique E1−E2 interaction required for optimal
conjugation of the ubiquitin-like protein NEDD8. *Nat Struct Mol
Biol* 2004;**11**:927−35.

124. Durfee LA, Kelley ML, Huibregtse JM. The basis for selective
E1−E2 interactions in the ISG15 conjugation system. *J Biol Chem*
2008;**283**:23895−902.

125. Jin J, Li X, Gygi SP, Harper JW. Dual E1 activation systems for
ubiquitin differentially regulate E2 enzyme charging. *Nature* 2007;
447:1135−8.

126. Lee I, Schindelin H. Structural insights into E1-catalyzed ubiquitin
activation and transfer to conjugating enzymes. *Cell* 2008;**134**:
268−78.

127. Lois LM, Lima CD. Structures of the SUMO E1 provide mechanistic
insights into SUMO activation and E2 recruitment to E1. *EMBO J*
2005;**24**:439−51.

128. Walden H, Podgorski MS, Schulman BA. Insights into the ubiquitin
transfer cascade from the structure of the activating enzyme for
NEDD8. *Nature* 2003;**422**:330−4.

129. Zhou W, Xu J, Li H, Xu M, Chen ZJ, Wei W, et al. Neddylation E2
UBE2F promotes the survival of lung cancer cells by activating
CRL5 to degrade NOXA *via* the K11 linkage. *Clin Cancer Res* 2017;
23:1104−16.

130. Ceccarelli DF, Tang X, Pelletier B, Orlicky S, Xie W, Plantevin V,
et al. An allosteric inhibitor of the human Cdc34 ubiquitin-
conjugating enzyme. *Cell* 2011;**145**:1075−87.

131. Huang H, Ceccarelli DF, Orlicky S, St-Cyr DJ, Ziemba A, Garg P,
et al. E2 enzyme inhibition by stabilization of a low-affinity interface
with ubiquitin. *Nat Chem Biol* 2014;**10**:156−63.

132. Ito T, Ando H, Suzuki T, Ogura T, Hotta K, Imamura Y, et al.
Identification of a primary target of thalidomide teratogenicity. *Sci-
ence* 2010;**327**:1345−50.

133. Aghajan M, Jonai N, Flick K, Fu F, Luo M, Cai X, et al. Chemical
genetics screen for enhancers of rapamycin identifies a specific in-
hibitor of an SCF family E3 ubiquitin ligase. *Nat Biotechnol* 2010;
28:738−42.

134. Chen BB, Coon TA, Glasser JR, McVerry BJ, Zhao J, Zhao Y, et al. A combinatorial F box protein directed pathway controls TRAF adaptor stability to regulate inflammation. *Nat Immunol* 2013;**14**:470−9.

135. Chan CH, Morrow JK, Li CF, Gao Y, Jin G, Moten A, et al. Pharmacological inactivation of Skp2 SCF ubiquitin ligase restricts cancer stem cell traits and cancer progression. *Cell* 2013;**154**:556−68.

136. Abed DA, Goldstein M, Albanyan H, Jin H, Hu L. Discovery of direct inhibitors of Keap1−Nrf2 protein−protein interaction as potential therapeutic and preventive agents. *Acta Pharm Sin B* 2015;**5**(4):285−99.

137. Liu Y, Wang X, Wang G, Yang Y, Yuan Y, Ouyang L. The past, present and future of potential small-molecule drugs targeting p53-MDM2/MDMX for cancer therapy. *Eur J Med Chem* 2019;**176**:92−104.

138. Chasapis CT, Spyroulias GA. RING finger E3 ubiquitin ligases: structure and drug discovery. *Curr Pharm Des* 2009;**15**:3716−31.

139. Huang X, Dixit VM. Drugging the undruggables: exploring the ubiquitin system for drug development. *Cell Res* 2016;**26**:484−98.

140. Xirodimas DP, Sundqvist A, Nakamura A, Shen L, Botting C, Hay RT. Ribosomal proteins are targets for the NEDD8 pathway. *EMBO Rep* 2008;**9**:280−6.

141. Jones J, Wu K, Yang Y, Guerrero C, Nillegoda N, Pan ZQ, et al. A targeted proteomic analysis of the ubiquitin-like modifier nedd8 and associated proteins. *J Proteome Res* 2008;**7**:1274−87.

142. Pan ZQ, Kentsis A, Dias DC, Yamoah K, Wu K. Nedd8 on cullin: building an expressway to protein destruction. *Oncogene* 2004;**23**:1985−97.

143. Blundell TL, Burke DF, Chirgadze D, Dhanaraj V, Hyvönen M, Innis CA, et al. Protein−protein interactions in receptor activation and intracellular signalling. *Biol Chem* 2000;**381**:955−9.

144. Sheng C, Dong G, Miao Z, Zhang W, Wang W. State-of-the-art strategies for targeting protein−protein interactions by small-molecule inhibitors. *Chem Soc Rev* 2015;**44**:8238−59.

145. Mathis. HTRF® technology. *J Biomol Screen* 1999;**4**:309−13.

146. Bazin H, Trinquet E, Mathis G. Time resolved amplification of cryptate emission: a versatile technology to trace biomolecular interactions. *Rev Mol Biotechnol* 2002;**82**:233−50.

147. Selvin PR. Principles and biophysical applications of lanthanide-based probes. *Annu Rev Biophys Biomol Struct* 2002;**31**:275−302.

148. Mathis G. Probing molecular interactions with homogeneous techniques based on rare earth cryptates and fluorescence energy transfer. *Clin Chem* 1995;**41**:1391−7.

149. Degorce F, Card A, Soh S, Trinquet E, Knapik GP, Xie B. HTRF: a technology tailored for drug discovery−a review of theoretical aspects and recent applications. *Curr Chem Genomics* 2009;**3**:22−32.

150. Wu K, Chong RA, Yu Q, Bai J, Spratt DE, Ching K, et al. Suramin inhibits cullin-RING E3 ubiquitin ligases. *Proc Natl Acad Sci U S A* 2016;**113**:E2011−8.

151. Janzen WP. High throughput screening. In: Walker JM, Rapley R, editors. *Molecular biomethods handbook*. 2nd ed. Totowa: Humana Press; 2008. p. 1097−118.

152. Hyer ML, Milhollen MA, Ciavarri J, Fleming P, Traore T, Sappal D, et al. A small-molecule inhibitor of the ubiquitin activating enzyme for cancer treatment. *Nat Med* 2018;**24**:186−93.

153. Slater O, Kontoyianni M. The compromise of virtual screening and its impact on drug discovery. *Expert Opin Drug Discovery* 2019;**14**:619−37.

154. Wingert BM, Camacho CJ. Improving small molecule virtual screening strategies for the next generation of therapeutics. *Curr Opin Chem Biol* 2018;**44**:87−92.

155. Hutter MC. The current limits in virtual screening and property prediction. *Future Med Chem* 2018;**10**:1623−35.

156. Wei D, Sun Y. Small RING finger proteins RBX1 and RBX2 of SCF E3 ubiquitin ligases: the role in cancer and as cancer targets. *Genes Cancer* 2010;**1**:700−7.

157. Baell JB, Holloway GA. New substructure filters for removal of pan assay interference compounds (PAINS) from screening libraries and for their exclusion in bioassays. *J Med Chem* 2010;**53**:2719−40.

158. Sushko I, Novotarskyi S, Körner R, Pandey AK, Rupp M, Teetz W, et al. Online chemical modeling environment (OCHEM): web platform for data storage, model development and publishing of chemical information. *J Comput Aided Mol Des* 2011;**25**:533−54.

159. Sushko I, Salmina E, Potemkin VA, Poda G, Tetko IV. ToxAlerts: a web server of structural alerts for toxic chemicals and compounds with potential adverse reactions. *J Chem Inf Model* 2012;**52**:2310−6.

160. Schorpp K, Rothenaigner I, Salmina E, Reinshagen J, Low T, Brenke JK, et al. Identification of small-molecule frequent hitters from AlphaScreen high-throughput screens. *J Biomol Screen* 2014;**19**:715−26.

161. Capuzzi SJ, Muratov EN, Tropsha A. Phantom PAINS: problems with the utility of alerts for Pan-assay interference compound. *J Chem Inf Model* 2017;**57**:417−27.